

Submodular Benchmark Selection

Alex Smola

Boson AI
4677 Old Ironsides Dr
Santa Clara CA 95054
smola@boson.ai

Evaluating large language models across many benchmarks is expensive, yet many benchmarks are highly correlated. We formalize the selection of a small, informative subset as submodular maximization under a multivariate Gaussian model. Entropy (log-determinant covariance) and mutual information between selected and remaining benchmarks arise as natural objectives. Both are submodular; entropy selection coincides with pivoted Cholesky and connects to spectral residual diagnostics, while mutual information is non-monotone in general but empirically monotone for small subsets, so we optimize it greedily. Experiments on three matrices from ten public leaderboards show that mutual information selection outperforms entropy for imputation at small subsets.

Code: <https://github.com/smolix/benchmark-selection>

1 Introduction

Evaluating language models comprehensively requires running them on a large and growing set of benchmarks. Each evaluation consumes compute, time, and human effort, yet many benchmarks are highly correlated: strong performance on one often predicts strong performance on another. This redundancy suggests that a small, well-chosen subset should capture most of the information in the full set, but which subset, and how small?

We formalize this as a submodular optimization problem. Given a score matrix of M models evaluated on N benchmarks, we model scores as draws from a multivariate Gaussian and select a subset \mathcal{A} of benchmarks to maximize either the entropy $H(X_{\mathcal{A}})$ or the mutual information $I(X_{\mathcal{A}}; X_{\bar{\mathcal{A}}})$. Both objectives are submodular Guestrin et al. [2005]. Entropy greedy is pivoted Cholesky, runs in $O(k^2 N)$ time, and provides a residual-variance diagnostic tied to the covariance spectrum. MI is non-monotone in general but empirically monotone for small k , so we use greedy as a heuristic rather than invoking the standard monotone-submodular guarantee. The MI variant combines forward Cholesky updates with complement refactorization; a stable implementation costs $O(kN^3)$, which is acceptable for hundreds of benchmarks. When shifted entropy is monotone, budget constraints can be handled via the modified greedy of Krause and Guestrin [2005]; for MI we use the same gain-per-cost idea as a heuristic.

Two practical challenges arise. First, score matrices are often incomplete, since not every model has been run on every benchmark. We handle this via EM for Gaussian missing data, estimating the covariance from partially observed entries. Second, practitioners need to know *how many* benchmarks to select. We compare the greedy residual trace with the eigenvalue decay of the score covariance Harbrecht et al. [2012]: fast empirical spectral decay provides a useful diagnostic for when small benchmark subsets are likely to work well.

Given the selected subset, unobserved scores are imputed via Gaussian conditional expectations. The choice of objective matters: mutual information selection outperforms entropy for imputation at small subset sizes, though entropy recovers and overtakes for larger subsets on well-conditioned datasets. This “surrogate gap” arises because entropy rewards benchmarks that are diverse from each other, while MI rewards coupling with the unselected complement, which drives imputation quality.

Related work. The benchmark landscape is vast: comprehensive suites such as HELM Liang et al. [2023] and the OPEN LLM LEADERBOARD Open LLM Leaderboard Team [2024] evaluate models on dozens of

tasks, while targeted benchmarks like MMLU Hendrycks et al. [2021a] and MTEB Muennighoff et al. [2023] provide fine-grained per-subject or per-task scores (see Appendix A for an in-depth review). A growing body of work has observed that many of these evaluations provide redundant signals: TINYBENCHMARKS Polo et al. [2024] reduces redundancy *within* a benchmark by selecting representative examples, SLOTH Polo et al. [2025] learns low-dimensional latent skills to predict performance across benchmark families, and BENCHBENCH Perlitz et al. [2024] diagnoses agreement among benchmarks via meta-benchmarking. Our approach is complementary: it is information-theoretic and prescriptive, telling practitioners which *entire benchmarks* to run and imputing scores for the rest, without training a predictive model beyond covariance estimation; entropy selection is also exactly pivoted Cholesky. This differs from BenchPress BenchPress contributors [2026], which empirically observes that benchmark scores can be interpolated.

Contributions. We design an end-to-end pipeline for benchmark selection:

1. Two submodular objectives (entropy, mutual information) with efficient, numerically stable greedy algorithms (Sections 3–4);
2. EM-based covariance estimation for incomplete score matrices (Section 3);
3. A spectral diagnostic using eigenvalue decay and the pivoted-Cholesky residual trace (Lemma 1);
4. Experiments on three score matrices from ten public leaderboards, showing that MI selection yields imputation $R^2 \geq 0.9$ with 5 benchmarks on MMLU and dominates entropy at small subset sizes (Section 5).

We next review submodularity (Section 2), formulate benchmark selection (Section 3), derive the algorithms (Section 4), and report experiments (Section 5). Dataset curation, numerical details, EM, selection order, BenchPress, nonlinear imputation, and logit-space experiments are in the appendix.

2 Background

Let $\mathcal{V} = \{v_1, \dots, v_n\}$ be a finite ground set and $f : 2^{\mathcal{V}} \rightarrow \mathbb{R}$ a set function. We study the problem of maximizing f subject to a cardinality constraint:

$$\max_{S \subseteq \mathcal{V}} f(S) \quad \text{subject to} \quad |S| \leq k. \quad (1)$$

Definition 1 (Monotonicity and Submodularity)

A set function $f : 2^{\mathcal{V}} \rightarrow \mathbb{R}$ with $f(\emptyset) = 0$ is:

- **Monotone** if for all $A \subseteq B \subseteq \mathcal{V}$: $f(A) \leq f(B)$.
- **Submodular** (*diminishing returns property*) if for all $A \subseteq B \subseteq \mathcal{V}$ and $v \notin B$:

$$\Delta(v | A) := f(A \cup \{v\}) - f(A) \geq f(B \cup \{v\}) - f(B) =: \Delta(v | B).$$

2.1 Submodular Selection

The greedy algorithm starts with $S_0 = \emptyset$ and at each step $i = 1, \dots, k$ adds the element with the largest marginal gain: $v^* = \operatorname{argmax}_{v \in \mathcal{V} \setminus S_{i-1}} \Delta(v | S_{i-1})$.

Theorem 1 (Nemhauser et al. [1978]) *Let f be monotone submodular with $f(\emptyset) = 0$, and let S^* be optimal for (1). Then the greedy solution S_G satisfies:*

$$f(S_G) \geq (1 - 1/e) \cdot f(S^*) \approx 0.632 \cdot f(S^*).$$

Feige [1998] showed that achieving an approximation ratio better than $(1 - 1/e)$ is NP-hard for general monotone submodular maximization under a cardinality constraint (assuming $P \neq NP$). The greedy algorithm is therefore essentially the best possible polynomial-time algorithm.

2.2 From Sensor Placement to Benchmark Selection

Our approach builds directly on the Gaussian process sensor placement framework of Guestrin et al. [2005]. In their setting, one selects k sensor locations from a set $\mathcal{V} = \{1, \dots, n\}$ to be maximally informative about

the unobserved locations, under a jointly Gaussian model $X_{\mathcal{V}} \sim \mathcal{N}(\mathbf{0}, \Sigma_{\mathcal{V}})$. Two objectives are natural: the *entropy*

$$f_1(S) = H(X_S) = \frac{1}{2} \log \det(2\pi e \Sigma_{SS}), \quad (2)$$

which measures the joint uncertainty of the selected sensors, and the *mutual information*

$$f_2(S) = I(X_S; X_{\mathcal{V} \setminus S}), \quad (3)$$

which measures how much observing S reduces uncertainty about the remaining locations.

Theorem 2 (Guestrin et al. [2005]) *For a multivariate Gaussian distribution:*

- (a) $H(X_S)$ is submodular in S . It is monotone when every one-step conditional entropy is non-negative, i.e., when all conditional variances exceed $(2\pi e)^{-1}$. Since differential entropy depends on scale, a fixed-cardinality objective can be shifted by a modular term to make these marginals non-negative without changing greedy choices.
- (b) The mutual information $I(X_S; X_{\mathcal{V} \setminus S})$ is non-negative and submodular in S , but non-monotone in general.

Where Guestrin et al. [2005] place sensors at spatial locations, we select benchmarks from a candidate set; where they observe data at the chosen locations, we evaluate models on the chosen benchmarks; where they predict unobserved readings, we impute unobserved benchmark scores.

A key difference, however, is that in the sensor placement setting each location is observed only once: the covariance Σ is a prior, typically derived from a Gaussian process kernel, and the algorithm must commit to sensor locations before any data is collected. In our setting we have access to a *score matrix* of M models already evaluated on N benchmarks, which provides M independent draws from the joint distribution. This means we can *estimate* Σ from data rather than specifying it a priori; the estimate improves as more models are evaluated.

3 Problem Formulation

We have M models and N benchmarks. Let $B \in \mathbb{R}^{M \times N}$ be the score matrix where B_{ij} is the score of model i on benchmark j . We treat each row as an independent draw from a multivariate Gaussian:

$$B_{i\cdot} \sim \mathcal{N}(\mu, \Sigma) \text{ for } i = 1, \dots, M, \quad (4)$$

where $\mu \in \mathbb{R}^N$ is the mean score vector and $\Sigma \in \mathbb{R}^{N \times N}$ is the covariance matrix. Writing $\mathbf{1}_M$ for the all-ones vector in \mathbb{R}^M , both are estimated from the data in matrix form:

$$\hat{\mu} = \frac{1}{M} B^\top \mathbf{1}_M \text{ and } \hat{\Sigma} = \frac{1}{M-1} \bar{B}^\top \bar{B} \text{ where } \bar{B} = B - \mathbf{1}_M \hat{\mu}^\top. \quad (5)$$

Score Imputation We want to choose a subset $\mathcal{A} \subseteq \{1, \dots, N\}$ of benchmarks to actually run. For a new model i , we observe only $B_{i\mathcal{A}}$ and must *impute* the remaining scores $B_{i\bar{\mathcal{A}}}$ where $\bar{\mathcal{A}} = \mathcal{V} \setminus \mathcal{A}$.

Under the Gaussian model, the conditional distribution of the unobserved scores given the observed scores is:

$$\mathbb{E}[B_{i\bar{\mathcal{A}}} | B_{i\mathcal{A}}] = \mu_{\bar{\mathcal{A}}} + \Sigma_{\bar{\mathcal{A}}\mathcal{A}} \Sigma_{\mathcal{A}\mathcal{A}}^{-1} (B_{i\mathcal{A}} - \mu_{\mathcal{A}}), \quad (6)$$

$$\text{Cov}(B_{i\bar{\mathcal{A}}} | B_{i\mathcal{A}}) = \Sigma_{\bar{\mathcal{A}}\bar{\mathcal{A}}} - \Sigma_{\bar{\mathcal{A}}\mathcal{A}} \Sigma_{\mathcal{A}\mathcal{A}}^{-1} \Sigma_{\mathcal{A}\bar{\mathcal{A}}}. \quad (7)$$

The conditional covariance depends only on the benchmarks in \mathcal{A} , not on the observed values.

Objective Function We instantiate the two objectives from Section 2.2 in the benchmark selection setting. Write $\mathcal{A} \subseteq \{1, \dots, N\}$ for the selected set and $\bar{\mathcal{A}} = \mathcal{V} \setminus \mathcal{A}$ for its complement.

Entropy Maximizing the entropy of the selected benchmarks is equivalent to maximizing $\log \det(\Sigma_{\mathcal{A}\mathcal{A}})$, since additive constants do not affect the argmax. For a fixed cardinality, the chain rule gives $H(X_{\mathcal{A}}) + H(X_{\bar{\mathcal{A}}} | X_{\mathcal{A}}) = H(X_{\mathcal{V}})$, so maximizing selected-set entropy is equivalent to minimizing the conditional entropy of the complement under the Gaussian model. This is a residual-uncertainty criterion, distinct from directly maximizing the coupling between selected and unselected benchmarks.

Mutual information. When the goal is to maximize the information that the selected benchmarks provide about the *remaining* ones, the natural objective is

$$\begin{aligned} f_2(\mathcal{A}) &= I(X_{\mathcal{A}}; X_{\bar{\mathcal{A}}}) = H(X_{\mathcal{A}}) + H(X_{\bar{\mathcal{A}}}) - H(X_{\mathcal{V}}) \\ &= \frac{1}{2} [\log \det \Sigma_{\mathcal{A}\mathcal{A}} + \log \det \Sigma_{\bar{\mathcal{A}}\bar{\mathcal{A}}} - \log \det \Sigma_{\mathcal{V}\mathcal{V}}]. \end{aligned} \quad (8)$$

The marginal gain of adding benchmark v to \mathcal{A} is (writing $\bar{\mathcal{A}}_v = \mathcal{V} \setminus (\mathcal{A} \cup \{v\})$):

$$\Delta(v | \mathcal{A}) = H(X_v | X_{\mathcal{A}}) - H(X_v | X_{\bar{\mathcal{A}}_v}) = \frac{1}{2} [\log \sigma_{v|\mathcal{A}}^2 - \log \sigma_{v|\bar{\mathcal{A}}_v}^2]. \quad (9)$$

By Theorem 2b, f_2 is submodular but not monotone, so the $(1 - 1/e)$ guarantee of standard greedy does not apply. However, for $k \ll N$ the MI gain $\Delta(v | \mathcal{A})$ remains positive at each step in all our experiments, and greedy MI consistently outperforms entropy for imputation at small k .

Total residual variance. A third option is to minimize $\sum_{j \notin \mathcal{A}} \sigma_{j|\mathcal{A}}^2 = \text{tr}(\Sigma_{\bar{\mathcal{A}}|\mathcal{A}})$, which targets average prediction accuracy. This objective is neither submodular nor supermodular in general, but greedy entropy gives a tractable pivoted-Cholesky surrogate whose residual trace can be monitored directly.

Handling Missing Entries In practice the score matrix may be incomplete. We use EM for Gaussian missing data Dempster et al. [1977], treating missing entries as latent variables under the MAR assumption Rubin [1976]. The E-step imputes via (6)–(7); the M-step re-estimates (μ, Σ) with a correction for imputation uncertainty. Appendix G gives initialization, convergence, and rank-deficient regularization. Since leaderboard missingness is often model- and benchmark-dependent, MAR is a working approximation.

4 Algorithms and Approximation Guarantees

4.1 Entropy Maximization

Cardinality constraint. Given the estimated covariance $\Sigma \in \mathbb{R}^{N \times N}$, select exactly k benchmarks maximizing $f_1(\mathcal{A}) = H(X_{\mathcal{A}})$. The greedy algorithm adds the benchmark with largest conditional variance at each step. Conditional variances are maintained via incremental Cholesky updates: each step computes $\ell_{j,t}$ from stored Cholesky rows and downdates the residual diagonal $d_j \leftarrow d_j - \ell_{j,t}^2$.

Algorithm 1 Greedy Entropy Maximization

Require: Covariance $\Sigma \in \mathbb{R}^{N \times N}$, cardinality k

Ensure: $\mathcal{A} \subseteq \mathcal{V}$ with $|\mathcal{A}| = k$

$\mathcal{A} \leftarrow \emptyset$

$d_j \leftarrow \Sigma_{jj}$ for all $j \in \mathcal{V}$

▷ residual diagonal

$\ell_{j,\cdot} \leftarrow ()$ for all $j \in \mathcal{V}$

▷ Cholesky rows

for $t = 1, \dots, k$ **do**

$j^* \leftarrow \operatorname{argmax}_{j \in \mathcal{V} \setminus \mathcal{A}} d_j$

$\mathcal{A} \leftarrow \mathcal{A} \cup \{j^*\}$

for $j \in \mathcal{V} \setminus \mathcal{A}$ **do**

$\ell_{j,t} \leftarrow (\Sigma_{j,j^*} - \ell_j^\top \ell_{j^*}) / \sqrt{d_{j^*}}$

$d_j \leftarrow d_j - \ell_{j,t}^2$

end for

end for

Return \mathcal{A}

4.2 Mutual Information Maximization

For the mutual information objective $f_2(\mathcal{A}) = I(X_{\mathcal{A}}; X_{\bar{\mathcal{A}}})$, the marginal gain (9) involves two conditional variances: $\sigma_{v|\mathcal{A}}^2$ (conditioning set grows) and $\sigma_{v|\bar{\mathcal{A}}_v}^2$ (conditioning set shrinks). The first is maintained by incremental Cholesky exactly as in Algorithm 1. For the second, we compute the complement precision diagonal $P_{vv} = [(\Sigma_{\bar{\mathcal{A}}\bar{\mathcal{A}}})^{-1}]_{vv}$. While a rank-1 downdate of the precision matrix exists, it is numerically unstable. Since the matrices are comparatively tiny, we perform a fresh Cholesky factorization of the complement block at each step, thus keeping numerical stability with minimal time overhead (see Appendix B for details).

Algorithm 2 Greedy Mutual Information Maximization

Require: Covariance $\Sigma \in \mathbb{R}^{N \times N}$, cardinality k

Ensure: $\mathcal{A} \subseteq \mathcal{V}$ with $|\mathcal{A}| = k$

```
 $\mathcal{A} \leftarrow \emptyset$ 
 $d_j \leftarrow \Sigma_{jj}$  for all  $j$  ▷ forward conditional variance
 $\ell_{j,\cdot} \leftarrow ()$  for all  $j$  ▷ Cholesky rows
for  $t = 1, \dots, k$  do
   $\bar{\mathcal{A}} \leftarrow \mathcal{V} \setminus \mathcal{A}$ 
   $L_{\bar{\mathcal{A}}} L_{\bar{\mathcal{A}}}^\top \leftarrow \Sigma_{\bar{\mathcal{A}}, \bar{\mathcal{A}}}$  ▷ fresh Cholesky of complement
   $P_{jj} \leftarrow \|(L_{\bar{\mathcal{A}}}^{-1})_{:,j}\|^2$  for all  $j \in \bar{\mathcal{A}}$  ▷ precision diagonal
   $j^* \leftarrow \operatorname{argmax}_{j \in \bar{\mathcal{A}}} \frac{1}{2} [\log d_j + \log P_{jj}]$ 
   $\mathcal{A} \leftarrow \mathcal{A} \cup \{j^*\}$ 
Cholesky update:
for  $j \in \mathcal{V} \setminus \mathcal{A}$  do
   $\ell_{j,t} \leftarrow (\Sigma_{j,j^*} - \ell_j^\top \ell_{j^*}) / \sqrt{d_{j^*}}$ 
   $d_j \leftarrow d_j - \ell_{j,t}^2$ 
end for
end for
Return  $\mathcal{A}$ 
```

4.3 Spectral Diagnostic

Let $\lambda_1 \geq \lambda_2 \geq \dots \geq \lambda_N$ be the eigenvalues of Σ . The truncated eigendecomposition gives the best rank- k approximation; its residual trace, equivalently the PCA residual variance, is $\sum_{j>k} \lambda_j$ (while the squared Frobenius residual is $\sum_{j>k} \lambda_j^2$). No selection of k benchmark coordinates can achieve a smaller total residual variance than this unconstrained rank- k benchmark, so the eigenvalue tail provides a lower bound on the residual variance of any benchmark subset of size k .

Harbrecht et al. [2012] give trace-norm convergence results for pivoted Cholesky under eigenvalue decay assumptions. We use this connection as a diagnostic rather than as a pointwise near-best bound: rapid eigenvalue decay suggests that a coordinate subset chosen by pivoted Cholesky should leave little residual variance, while the actual residual trace is measured in the experiments. The key observation is that Algorithm 1 is exactly pivoted Cholesky: the greedy entropy criterion $\operatorname{argmax}_j d_j$ selects the pivot with maximum residual diagonal, since $\Delta(j | \mathcal{A}) = \frac{1}{2} \log(2\pi e d_j)$ is monotone in d_j . If one wants a monotone-submodular approximation statement, it applies to any modularly shifted entropy objective $H_c(X_S) = H(X_S) + c|S|$ whose one-step marginals are non-negative; this shift leaves the fixed-cardinality greedy choices unchanged.

Lemma 1 (Greedy approximation and residual identity) *Let $\Sigma \in \mathbb{R}^{N \times N}$ be positive definite with eigenvalues $\lambda_1 \geq \dots \geq \lambda_N > 0$, and let \mathcal{A}_G be the k -element set returned by Algorithm 1. Then:*

- (a) *Let c be any constant such that $H_c(X_S) := H(X_S) + c|S|$ is monotone. Since the added term is modular, it shifts every one-step marginal by the same constant and therefore does not change the greedy choices under a fixed-cardinality budget. Algorithm 1 satisfies*

$$H_c(X_{\mathcal{A}_G}) \geq (1 - 1/e) \cdot \max_{|\mathcal{A}|=k} H_c(X_{\mathcal{A}}).$$

- (b) *The residual variance after selection is the trace of the pivoted-Cholesky residual:*

$$\operatorname{tr}(\Sigma_{\bar{\mathcal{A}}_G | \mathcal{A}_G}) = \operatorname{tr}(\Sigma - L_k L_k^\top).$$

Thus the eigenvalue tail is an unconstrained lower bound and the pivoted-Cholesky residual gives the corresponding coordinate-selection diagnostic.

5 Experiments

For a realistic analysis, we assemble score matrices from ten public leaderboards (Appendix A). Two leaderboards are usable outright (MMLU and MTEB); the rest are combined, with a subset of MMLU, into a

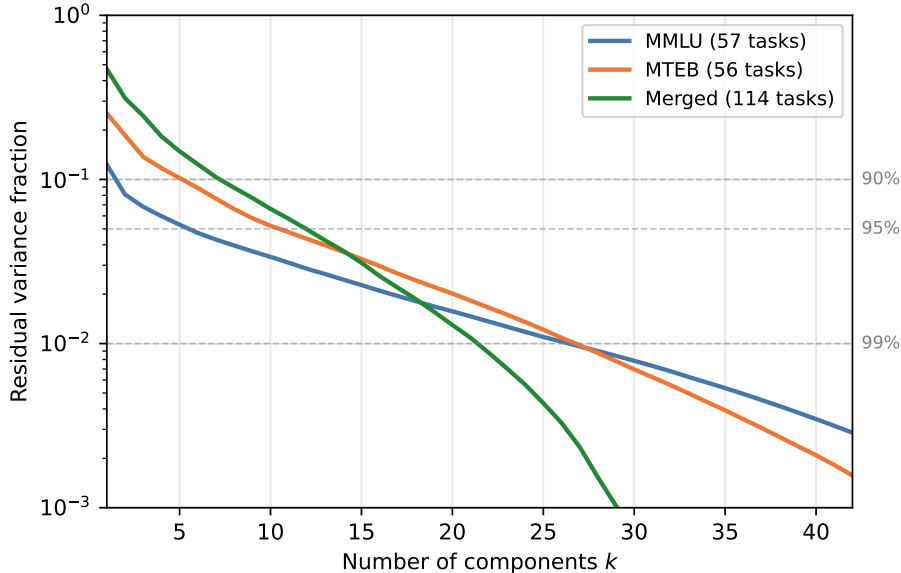


Figure 1: Residual variance fraction $1 - \rho(k)$ of the correlation matrix for each experiment matrix. Dashed lines mark 90%, 95%, and 99% explained variance.

sparse model-by-benchmark matrix. We obtain: MMLU ($5,452 \times 57$, fully observed), MTEB (263×56 , 77% observed), and MERGED (118×114 , 31% observed), combining all collections except MTEB via model canonicalization (Appendix E). For MERGED, we keep score-like quantities and drop auxiliary count, uncertainty, and length fields. Table 1 summarizes this.

5.1 Protocol

All experiments use 10-fold cross-validation: the M models are randomly permuted and partitioned into $K = 10$ balanced folds (sizes differing by at most 1). Each fold serves once as the *validation* set ($\approx M/10$ models). For the remaining $9M/10$ models (the *pool*), we subsample a training set of size $\lfloor (1-p)M \rfloor$ via a second random permutation, where $p \in \{10\%, 20\%, 50\%, 90\%\}$ is the holdout fraction. At $p = 10\%$ the training set equals the full pool; at $p = 90\%$ it contains roughly $M/10$ models, testing whether a handful of training models suffice. The covariance is estimated from the training set, the greedy algorithm selects \mathcal{A} , and the validation models’ unselected scores are imputed via Gaussian conditional expectations. Covariance estimation uses pairwise correlations for fully observed matrices (MMLU) and the EM algorithm of Appendix G for matrices with substantial missingness (MTEB, MERGED). Before imputation, scores are standardized using training-set means and standard deviations. Conditional solves use a ridge term $10^{-2}I$ for numerical stability, and standardized validation scores are clipped to $[-10, 10]$ before computing errors. The reported R^2 is computed in this standardized space, so predicting zero corresponds to predicting the training-set mean for each benchmark. For sparse matrices, validation rows need not contain every selected benchmark. We therefore condition only on selected benchmarks observed for that validation model and evaluate only observed unselected scores. We test prediction from existing leaderboard coverage rather than simulating deployment, where all selected benchmarks would be newly run.

5.2 Eigenspectrum

For each score matrix we standardize columns to unit variance, estimate (μ, Σ) via the EM algorithm of Appendix G and convert $\hat{\Sigma}$ to a correlation matrix $R = D^{-1/2}\hat{\Sigma}D^{-1/2}$ where $D = \text{diag}(\hat{\Sigma})$. Figure 1 plots the residual variance fraction $1 - \rho(k)$ on a logarithmic scale, where $\rho(k) = \sum_{j \leq k} \lambda_j / \text{tr}(R)$ is the cumulative explained variance.

The key message is consistent across all three matrices: benchmark scores live in a low-dimensional subspace. MMLU is highly redundant (two components capture 90% of the variance across 57 subjects), MTEB requires six components for 90%, and MERGED requires eight components for 90% (twelve for 95%). The

latter remains sparse and needs PSD regularization during EM, but its spectrum still decays quickly. Since entropy greedy is pivoted Cholesky, the same low-rank structure suggests that its measured residual trace should fall quickly as benchmarks are selected. This supports the eigenspectrum as a subset-size diagnostic; cross-validation below is the main empirical evidence.

5.3 Imputation Quality vs. Subset Size

We run greedy entropy maximization (Algorithm 1) for $k = 1, \dots, 15$ selected benchmarks and evaluate imputation on held-out models at each step. As a baseline, we also evaluate *random selection*: for each fold, k benchmarks are chosen uniformly at random (a fresh permutation per fold), and the same Gaussian imputation is applied using the estimated covariance. Figures 2–4 show the mean and standard deviation across folds for each holdout fraction; dashed lines show the random baseline.

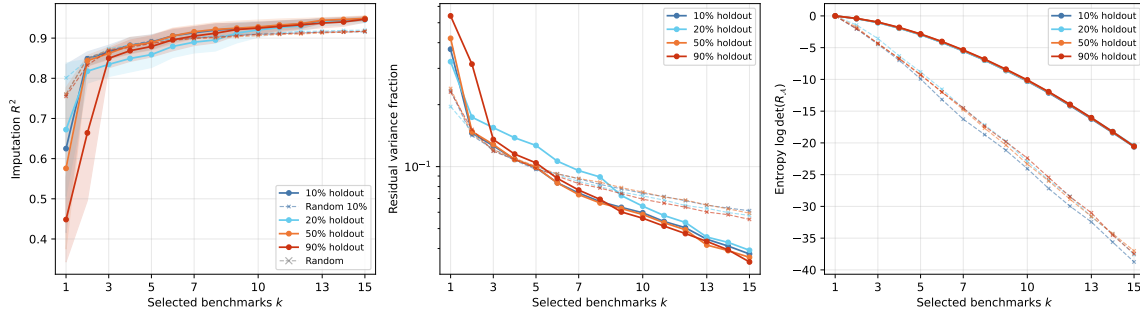


Figure 2: Cross-validation results for **MMLU** ($5\,452 \times 57$, fully observed). Left: imputation R^2 on held-out models. Center: residual variance fraction (semilog). Right: entropy of the selected submatrix. Solid lines: greedy entropy selection; dashed lines: random selection baseline. Shaded bands show ± 1 standard deviation across folds.

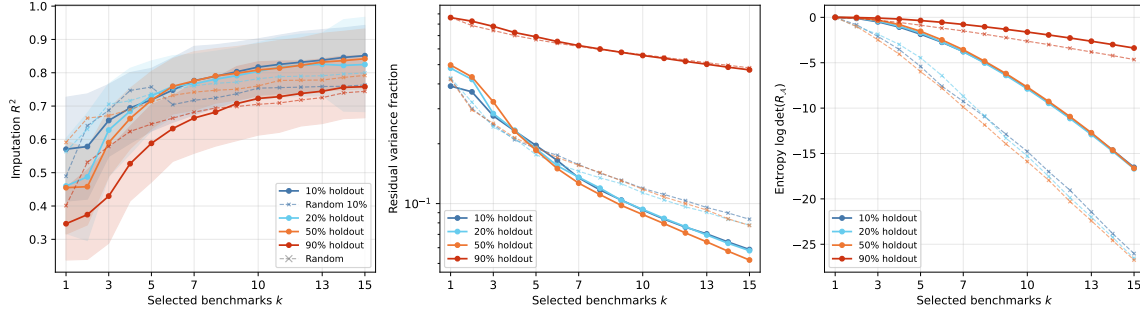


Figure 3: Cross-validation results for **MTEB** (263×56 , 77.3% observed).

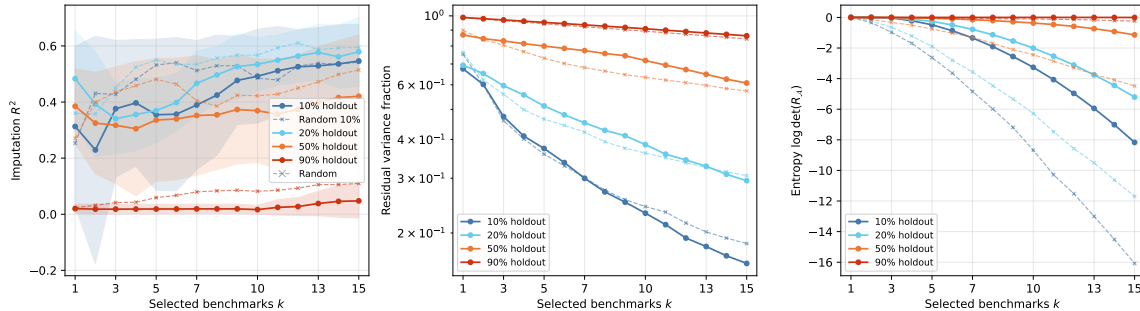


Figure 4: Cross-validation results for **MERGED** (118×114 , 31.1% observed).

On MMLU, with just $k = 5$ selected subjects the average imputation R^2 reaches 0.89; at $k = 10$ it exceeds 0.92; and at $k = 15$ it is 0.95. Performance is remarkably stable across holdout fractions: even with 90% (~ 545 training models), the R^2 at $k = 10$ remains 0.92. MTEB shows $R^2 \approx 0.72$ at $k = 5$ and ≈ 0.85

at $k = 15$ under 10%, with modest degradation for the 90%. MERGED is hardest ($R^2 \approx 0.55$ at $k = 15$), reflecting 68.9% missingness and heterogeneous benchmarks.

Random baseline. On MMLU, random selection is surprisingly competitive ($R^2 \approx 0.89$ at $k = 5$), reflecting the extreme redundancy of the 57 subjects. The gap widens for MTEB and MERGED, where greedy achieves substantially lower residual variance and higher entropy, suggesting that principled selection matters most when the benchmark space has multi-dimensional structure, although random selection remains a strong baseline for imputation.

Summary. Across all three matrices, a small number of carefully chosen benchmarks captures a disproportionate share of evaluative information. For the best-conditioned dataset (MMLU), 5 benchmarks out of 57 explain 89% of the variance; even for the challenging MERGED matrix, 15 benchmarks out of 114 explain more than half the variance in held-out data.

5.4 Entropy vs. Mutual Information

We now compare greedy entropy maximization (Algorithm 1) and greedy mutual information maximization (Algorithm 2), both against each other and against the random selection baseline. All three methods are evaluated under the same 10-fold CV protocol with 10% holdout. Figures 5–7 show three metrics for each method: imputation R^2 on held-out models (left), residual variance fraction (center), and the mutual information $I(X_{\mathcal{A}}; X_{\bar{\mathcal{A}}})$ achieved by each method’s selection (right).

Across all three datasets, MI selection yields higher imputation R^2 than entropy for small k . On MMLU, the gap is largest at $k = 1$ ($R^2 = 0.83$ vs. 0.65) and the two methods cross over around $k \approx 7$. On MTEB, MI leads by roughly 10 R^2 points for $k \leq 3$; on MERGED, MI’s advantage persists for larger k , reaching $R^2 \approx 0.59$ vs. 0.55 at $k = 15$. An instructive finding is the “surrogate gap” visible in the center panels: entropy achieves *lower* residual variance than MI, consistent with its pivoted-Cholesky residual trace diagnostic, yet for small k this does not translate into better imputation, as entropy measures the information of the benchmarks selected, rather than their value to predict the scores of the benchmarks left out. This arises because entropy rewards benchmarks that are *diverse from each other*, while MI additionally rewards coupling with the complement via the term $\log P_{jj}$ in (9). At small k , coupling with the complement matters most; as k grows, diversity suffices and entropy catches up.

Summary. MI selection provides a clear advantage for small k . For well-conditioned datasets, entropy overtakes MI for large k . The improvement from MI is largest and most persistent on the challenging MERGED dataset, consistent with its goal of finding benchmarks predictive of the remaining data. We recommend MI for small-budget score imputation, while entropy remains useful for diversity or residual-variance reduction. Formal normality tests (Appendix H) reject the Gaussian assumption on all datasets, yet the conditional mean, the best linear predictor regardless of the true distribution, yields accurate imputations throughout.

6 Discussion

We presented a principled approach to benchmark selection via submodular optimization. Entropy and MI are both submodular: entropy selection has shifted monotone-submodular guarantees and is exactly pivoted Cholesky, while MI is non-monotone in general and is optimized greedily as an empirical heuristic. Experiments on three matrices from ten public leaderboards show that MI improves imputation at small subsets, while entropy catches up for larger subsets. On MMLU, 5 MI-selected benchmarks out of 57 achieve imputation $R^2 = 0.91$; even a single benchmark reaches $R^2 = 0.83$.

Cost-aware selection. Benchmarks vary enormously in computational cost. Our framework can use a knapsack budget and select by gain per unit cost. For shifted entropy with non-negative marginals, this is the usual monotone-submodular knapsack setting; for MI, it is a practical heuristic unless one uses a dedicated non-monotone algorithm. A refined treatment would use measured compute or labeling costs.

Safety and fairness coverage. In practice, certain evaluation axes (safety, fairness, toxicity) must always be assessed regardless of statistical redundancy. This motivates constrained selection: maximize the submodular objective with specified benchmarks always included. Algorithmically, initialize \mathcal{A} with the mandatory benchmarks and run greedy on the rest.

Alternative approaches. We kept the main derivation focused on Gaussian imputation and linear regression. More complex selection and imputation methods are in the appendix, including the sparse BenchPress

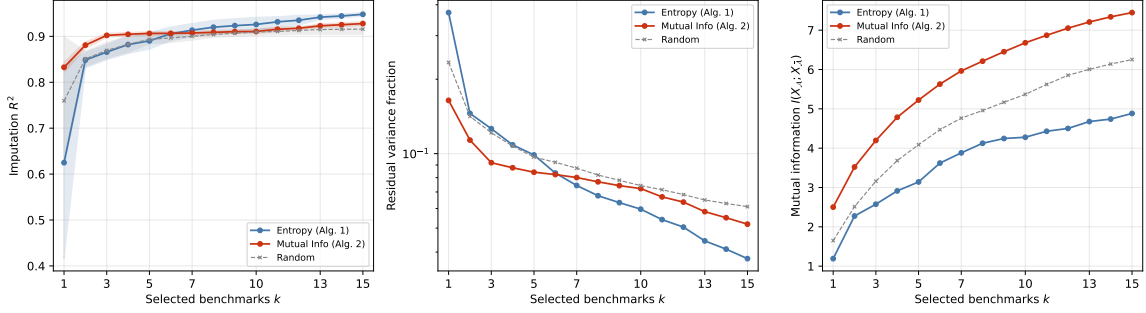


Figure 5: Entropy vs. MI vs. random selection on **MMLU**. MI achieves higher R^2 for small k despite higher residual variance, because it selects benchmarks coupled with the complement. The random baseline (gray dashed) is competitive in R^2 but achieves lower entropy and MI, confirming that Gaussian imputation is effective when the data is highly redundant.

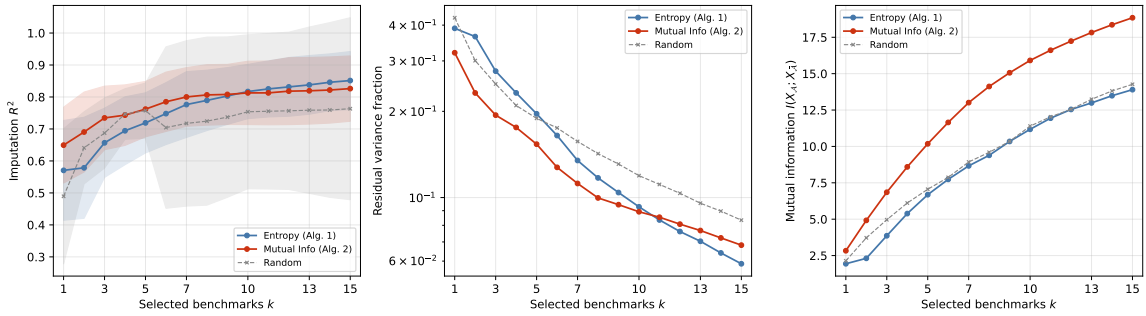


Figure 6: Entropy vs. MI vs. random selection on **MTEB**. MI leads for small k ($\sim 10 R^2$ points at $k \leq 3$), with entropy overtaking for $k \geq 10$. Random selection performs comparably in R^2 but is dominated in residual variance and MI.

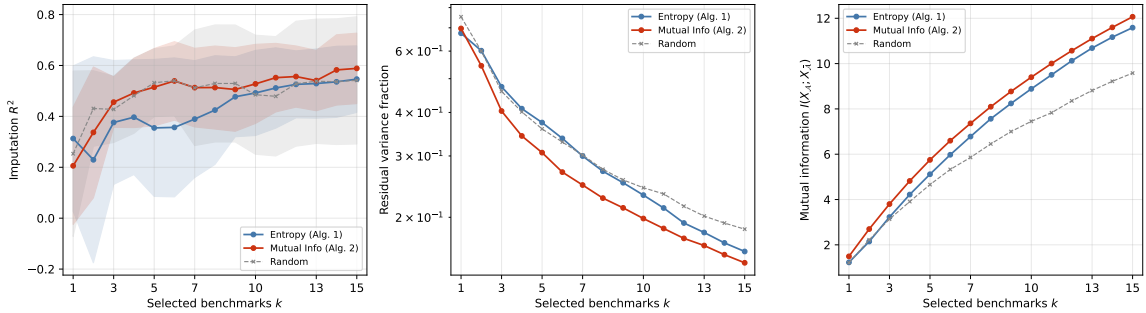


Figure 7: Entropy vs. MI vs. random selection on **MERGED**. MI provides a substantial advantage over entropy for large k . The random baseline is competitive with both methods in R^2 , reflecting the noisy covariance estimates in this sparse regime (31.1% observed).

dataset [BenchPress contributors, 2026] (Appendix I). The MERGED matrix is more useful for our main claims because it contains more benchmarks and models.

Replacing Gaussian conditional imputation with zero-shot TABIMPUTE [Feitelberg et al., 2025] reduces R^2 substantially (Appendix J), showing that estimated covariance provides stronger signal than in-context learning here. A logit-space score transform [BenchPress contributors, 2026] likewise fails to improve imputation (Appendix K), suggesting that the raw Gaussian framework captures the dominant linear structure.

Future work. Benchmark selection is the dual of model selection: transposing the score matrix lets us select *reference models* that characterize a new benchmark without evaluating the full model zoo. The optimal granularity of benchmarks (few large vs. many small) and robustness to benchmark-specific overfitting (e.g. fine-tuning on benchmark-adjacent data) remain open questions.

References

- Jacob Austin, Augustus Odena, Maxwell Nye, Maarten Bosma, Henryk Michalewski, David Dohan, Ellen Jiang, Carrie Cai, Michael Terry, Quoc Le, and Charles Sutton. Program synthesis with large language models. *arXiv preprint arXiv:2108.07732*, 2021.
- Yushi Bai, Xin Lv, Jiajie Zhang, Hongchang Lyu, Jiankai Tang, Zhidian Huang, Zhengxiao Du, Xiao Liu, Aohan Zeng, Lei Hou, Yuxiao Dong, Jie Tang, and Juanzi Li. LongBench: A bilingual, multitask benchmark for long context understanding. In *Proceedings of the 62nd Annual Meeting of the Association for Computational Linguistics*, 2024.
- BenchPress contributors. LLM Benchmark Matrix Completion. <https://github.com/anadim/llm-benchmark-matrix>, 2026. GitHub repository; includes the BenchPress method.
- Stella Biderman, Hailey Schoelkopf, Lintang Sutawika, Leo Gao, Jonathan Tow, Baber Abbasi, Alham Fikri Aji, Pawan Sasanka Ammanamanchi, Sidney Black, Jordan Clive, Anthony DiPofi, Julen Etxaniz, Benjamin Fattori, Jessica Zosa Forde, Charles Foster, Jeffrey Hsu, Mimansa Jaiswal, Wilson Y Lee, Haonan Li, Charles Lovering, Niklas Muennighoff, Ellie Pavlick, Jason Phang, Aviya Skowron, Samson Tan, Xiangru Tang, Kevin A Wang, Genta Indra Winata, François Yvon, and Andy Zou. Lessons from the trenches on reproducible evaluation of language models. *arXiv preprint arXiv:2405.14782*, 2024.
- Mark Chen, Jerry Tworek, Heewoo Jun, Qiming Yuan, Henrique Ponde de Oliveira Pinto, Jared Kaplan, Harrison Edwards, Yuri Burda, Nicholas Joseph, Greg Brockman, Alex Ray, Raul Puri, Gretchen Krueger, Michael Petrov, Heidy Khlaaf, Girish Sastry, Pamela Mishkin, Brooke Chan, Scott Gray, Nick Ryder, Mikhail Pavlov, Alethea Power, Lukasz Kaiser, Mohammad Bavarian, Clemens Winter, Philippe Tillet, Felipe Petroski Such, Dave Cummings, Matthias Plappert, Fotios Chantzis, Elizabeth Barnes, Ariel Herbert-Voss, William Hebggen Guss, Alex Nichol, Alex Paino, Nikolas Tezak, Jie Tang, Igor Babuschkin, Suchir Balaji, Shantanu Jain, William Saunders, Christopher Hesse, Andrew N Carr, Jan Leike, Josh Achiam, Vedavyas Misra, Evan Morikawa, Alec Radford, Matthew Knight, Miles Brundage, Mira Murati, Katie Mayer, Peter Welinder, Bob McGrew, Dario Amodei, Sam McCandlish, Ilya Sutskever, and Wojciech Zaremba. Evaluating large language models trained on code. *arXiv preprint arXiv:2107.03374*, 2021.
- Wei-Lin Chiang, Lianmin Zheng, Ying Sheng, Anastasios Nikolas Angelopoulos, Tianle Li, Dacheng Li, Banghua Zhu, Hao Zhang, Michael Jordan, Joseph E Gonzalez, and Ion Stoica. Chatbot arena: An open platform for evaluating LLMs by human preference. In *International Conference on Machine Learning*, 2024.
- Peter Clark, Isaac Cowhey, Oren Etzioni, Tushar Khot, Ashish Sabharwal, Carissa Schoenick, and Oyvind Tafjord. Think you have solved question answering? try ARC, the AI2 reasoning challenge. *arXiv preprint arXiv:1803.05457*, 2018.
- Karl Cobbe, Vineet Kosaraju, Mohammad Bavarian, Mark Chen, Heewoo Jun, Lukasz Kaiser, Matthias Plappert, Jerry Tworek, Jacob Hilton, Reiichiro Nakano, Christopher Hesse, and John Schulman. Training verifiers to solve math word problems. *arXiv preprint arXiv:2110.14168*, 2021.
- Arthur P. Dempster, Nan M. Laird, and Donald B. Rubin. Maximum likelihood from incomplete data via the EM algorithm. *Journal of the Royal Statistical Society: Series B (Methodological)*, 39(1):1–38, 1977.
- Yann Dubois, Balázs Galambosi, Percy Liang, and Tatsunori B Hashimoto. Length-controlled AlpacaEval: A simple way to debias automatic evaluators. In *Conference on Language Modeling*, 2024.
- Uriel Feige. A threshold of $\ln n$ for approximating set cover. *Journal of the ACM (JACM)*, 45(4):634–652, 1998.
- Jacob Feitelberg, Dwaipayan Saha, Kyuseong Choi, Zaid Ahmad, Anish Agarwal, and Raaz Dwivedi. TabImpute: Universal zero-shot imputation for tabular data. *arXiv preprint arXiv:2510.02625*, 2025.
- Gene H Golub and Charles F Van Loan. *Matrix Computations*. Johns Hopkins University Press, 4th edition, 2013.
- C. Guestrin, A. Krause, and A. Singh. Near-optimal sensor placements in gaussian processes. In *International Conference on Machine Learning ICML'05*, 2005.

- Helmut Harbrecht, Michael Peters, and Reinhold Schneider. On the low-rank approximation by the pivoted Cholesky decomposition. *Applied Numerical Mathematics*, 62(4):428–440, 2012.
- Dan Hendrycks, Collin Burns, Steven Basart, Andy Zou, Mantas Mazeika, Dawn Song, and Jacob Steinhardt. Measuring massive multitask language understanding. In *International Conference on Learning Representations*, 2021a.
- Dan Hendrycks, Collin Burns, Saurav Kadavath, Akul Arora, Steven Basart, Eric Tang, Dawn Song, and Jacob Steinhardt. Measuring mathematical problem solving with the MATH dataset. In *Advances in Neural Information Processing Systems*, 2021b.
- Cheng-Ping Hsieh, Simeng Sun, Samuel Kriman, Shantanu Acharya, Dima Rekesh, Fei Jia, Yang Zhang, and Boris Ginsburg. RULER: What’s the real context size of your long-context language models? *arXiv preprint arXiv:2404.06654*, 2024.
- Carlos E Jimenez, John Yang, Alexander Wettig, Shunyu Yao, Kexin Pei, Ofir Press, and Karthik Narasimhan. SWE-bench: Can language models resolve real-world GitHub issues? In *International Conference on Learning Representations*, 2024.
- A. Krause and C. Guestrin. A note on the budgeted maximization of submodular functions. CMU-CALD 05-103, CMU, 2005.
- Andreas Krause, Ajit Singh, and Carlos Guestrin. Near-optimal sensor placements in Gaussian processes: Theory, efficient algorithms and empirical studies. *Journal of Machine Learning Research*, 9:235–284, 2008.
- Olivier Ledoit and Michael Wolf. A well-conditioned estimator for large-dimensional covariance matrices. *Journal of Multivariate Analysis*, 88(2):365–411, 2004.
- Tianle Li, Wei-Lin Chiang, Evan Frick, Lisa Dunlap, Tianhao Wu, Banghua Zhu, Joseph E Gonzalez, and Ion Stoica. From crowdsourced data to high-quality benchmarks: Arena-Hard and BenchBuilder pipeline. *arXiv preprint arXiv:2406.11939*, 2024.
- Percy Liang, Rishi Bommasani, Tony Lee, Dimitris Tsipras, Dilara Soylu, Michihiro Yasunaga, Yian Zhang, Deepak Narayanan, Yuhuai Wu, Ananya Kumar, Benjamin Newman, Binhang Yuan, Bobby Yan, Ce Zhang, Christian Cosgrove, Christopher D Manning, Christopher Ré, Diana Acosta-Navas, Drew A Hudson, Eric Zelikman, Esin Durmus, Faisal Ladhak, Frieda Rong, Hongyu Ren, Huaxiu Yao, Jue Wang, Keshav Santhanam, Laurel Orr, Lucia Zheng, Mert Yuksekogonul, Mirac Suzgun, Nathan Kim, Neel Guha, Niladri Chatterji, Omar Khattab, Peter Henderson, Qian Huang, Ryan Chi, Sang Michael Xie, Shibani Santurkar, Surya Ganguli, Tatsunori Hashimoto, Thomas Icard, Tianyi Zhang, Vishrav Chaudhary, William Wang, Xuechen Li, Yifan Mai, Yuhui Zhang, and Yuta Koreeda. Holistic evaluation of language models. *Transactions on Machine Learning Research*, 2023.
- Bill Yuchen Lin, Yuntian Deng, Khyathi Chandu, Faeze Brahman, Abhilasha Ravichander, Valentina Pyatkin, Nouha Dziri, Ronan Le Bras, and Yejin Choi. WildBench: Benchmarking LLMs with challenging tasks from real users in the wild. *arXiv preprint arXiv:2406.04770*, 2024.
- Stephanie Lin, Jacob Hilton, and Owain Evans. TruthfulQA: Measuring how models mimic human falsehoods. In *Proceedings of the 60th Annual Meeting of the Association for Computational Linguistics*, 2022.
- Kanti V. Mardia. Measures of multivariate skewness and kurtosis with applications. *Biometrika*, 57(3): 519–530, 1970.
- Mantas Mazeika, Long Phan, Xuwang Yin, Andy Zou, Zifan Wang, Norman Mu, Elham Sakhaee, Nathaniel Li, Steven Basart, Bo Li, David Forsyth, and Dan Hendrycks. HarmBench: A standardized evaluation framework for automated red teaming and robust refusal. In *International Conference on Machine Learning*, 2024.
- Michel Minoux. Accelerated greedy algorithms for maximizing submodular set functions. In *Optimization Techniques (LNCS)*. Springer, 1978.
- Baharan Mirzasoleiman, Ashwinkumar Badanidiyuru, Amin Karbasi, Jan Vondrák, and Andreas Krause. Lazier than lazy greedy. In *Proceedings of the AAAI Conference on Artificial Intelligence*, 2015.

- Niklas Muennighoff, Nouamane Tazi, Loïc Magne, and Nils Reimers. MTEB: Massive text embedding benchmark. In *Proceedings of the 17th Conference of the European Chapter of the Association for Computational Linguistics*, pages 2014–2037, 2023.
- George L Nemhauser, Laurence A Wolsey, and Marshall L Fisher. An analysis of approximations for maximizing submodular set functions—I. *Mathematical Programming*, 14(1):265–294, 1978.
- Open LLM Leaderboard Team. Open LLM Leaderboard 2. <https://huggingface.co/collections/open-llm-leaderboard/open-llm-leaderboard-2>, 2024. Hugging Face collection.
- Alicia Parrish, Angelica Chen, Nikita Nangia, Vishakh Padmakumar, Jason Phang, Jessica Thompson, Phu Mon Htut, and Samuel R Bowman. BBQ: A hand-built bias benchmark for question answering. In *Findings of the Association for Computational Linguistics: ACL 2022*, 2022.
- Yotam Perlitz, Ariel Gera, Ofir Arviv, Asaf Yehudai, Elron Bandel, Eyal Shnarch, Michal Shmueli-Scheuer, and Leshem Choshen. Do these LLM benchmarks agree? fixing benchmark evaluation with BenchBench. *arXiv preprint arXiv:2407.13696*, 2024.
- Felipe Maia Polo, Lucas Weber, Leshem Choshen, Yuekai Sun, Gongjun Xu, and Mikhail Yurochkin. tiny-Benchmarks: Evaluating LLMs with fewer examples. In *International Conference on Machine Learning*, 2024.
- Felipe Maia Polo, Seamus Somerstep, Leshem Choshen, Yuekai Sun, and Mikhail Yurochkin. Sloth: Scaling laws for LLM skills to predict multi-benchmark performance across families. In *Advances in Neural Information Processing Systems*, 2025.
- David Rein, Betty Li Hou, Asa Cooper Stickland, Jackson Petty, Richard Yuanzhe Pang, Julien Dirani, Julian Michael, and Samuel R Bowman. GPQA: A graduate-level google-proof Q&A benchmark. In *First Conference on Language Modeling*, 2024.
- Donald B. Rubin. Inference and missing data. *Biometrika*, 63(3):581–592, 1976.
- Keisuke Sakaguchi, Ronan Le Bras, Chandra Bhagavatula, and Yejin Choi. WinoGrande: An adversarial winograd schema challenge at scale. In *Proceedings of the AAAI Conference on Artificial Intelligence*, 2020.
- S. S. Shapiro and M. B. Wilk. An analysis of variance test for normality (complete samples). *Biometrika*, 52(3–4):591–611, 1965.
- Zayne Sprague, Xi Ye, Kaj Bostrom, Swarat Chaudhuri, and Greg Durrett. MuSR: Testing the limits of chain-of-thought with multistep soft reasoning. In *International Conference on Learning Representations*, 2024.
- Aarohi Srivastava, Abhinav Rastogi, Abhishek Rao, et al. Beyond the imitation game: Quantifying and extrapolating the capabilities of language models. *Transactions on Machine Learning Research*, 2023.
- Maxim Sviridenko. A note on maximizing a submodular set function subject to a knapsack constraint. *Operations Research Letters*, 32(1):41–43, 2004.
- Yubo Wang, Xueguang Ma, Ge Zhang, Yuansheng Ni, Abhramil Chandra, Shiguang Guo, Weiming Ren, Aaran Arulraj, Xuan He, Ziyang Jiang, Tianle Li, Max Ku, Kai Wang, Alex Zhuang, Rongqi Fan, Xiang Yue, and Wenhu Chen. MMLU-Pro: A more robust and challenging multi-task language understanding benchmark. In *Advances in Neural Information Processing Systems*, 2024.
- Colin White, Samuel Dooley, Manley Roberts, Arka Pal, Ben Feuer, Siddhartha Jain, Ravid Shwartz-Ziv, Neel Jain, Khalid Saifullah, Sreemanti Dey, Shubh Agrawal, Sandeep Singh Sandha, Siddhartha Naidu, Chinmay Hegde, Yann LeCun, Tom Goldstein, Willie Neiswanger, and Micah Goldblum. LiveBench: A challenging, contamination-limited LLM benchmark. In *International Conference on Learning Representations*, 2025.
- Rowan Zellers, Ari Holtzman, Yonatan Bisk, Ali Farhadi, and Yejin Choi. HellaSwag: Can a machine really finish your sentence? In *Proceedings of the 57th Annual Meeting of the Association for Computational Linguistics*, 2019.

Lianmin Zheng, Wei-Lin Chiang, Ying Sheng, Siyuan Zhuang, Zhanghao Wu, Yonghao Zhuang, Zi Lin, Zhuohan Li, Dacheng Li, Eric P Xing, Hao Zhang, Joseph E Gonzalez, and Ion Stoica. Judging LLM-as-a-judge with MT-Bench and chatbot arena. In *Advances in Neural Information Processing Systems*, 2023.

Jeffrey Zhou, Tianjian Lu, Swaroop Mishra, Siddhartha Brahma, Sujoy Basu, Yi Luan, Denny Zhou, and Le Hou. Instruction-following evaluation for large language models. *arXiv preprint arXiv:2311.07911*, 2023.

Terry Yue Zhuo, Minh Chien Vu, Jenny Chim, Han Hu, Wenhao Yu, Ratnadira Widyasari, Imam Nur Bani Yusuf, Haolan Zhan, Junda He, Indraneil Paul, Simon Brunner, Chen Gong, Thong Hoang, Arnel Randy Zebaze, Xiaoheng Hong, Wen-Ding Li, Jean Kaddour, Ming Xu, Zhihan Zhang, Prateek Yadav, Naman Jain, Alex Gu, Zhoujun Cheng, Jiawei Liu, Qian Liu, Zijian Wang, Binyuan Hui, Niklas Muennighoff, David Lo, Daniel Fried, Xiaoning Du, Harm de Vries, and Leandro von Werra. BigCodeBench: Benchmarking code generation with diverse function calls and complex instructions. In *International Conference on Learning Representations*, 2025.

A The Benchmark Landscape

The rapid proliferation of large language models has been accompanied by an equally rapid expansion in evaluation benchmarks, creating a complex and often redundant assessment ecosystem.

Comprehensive evaluation suites. Several projects have attempted to unify LLM evaluation under a single umbrella. HELM Liang et al. [2023] evaluates models across 42 scenarios spanning 7 metric categories (accuracy, calibration, robustness, fairness, bias, toxicity, and efficiency), and its online platform has since grown to cover over 50 scenarios and 140 models. The OPEN LLM LEADERBOARD, hosted by Hugging Face, standardized public comparison; its v1 aggregated 6 benchmarks (ARC, HELLASWAG, MMLU, TRUTHFULQA, WINOGRANDE, GSM8K), while v2 (launched October 2024) replaced them with 6 harder alternatives: IFEVAL Zhou et al. [2023], BIG-BENCH HARD, MATH LEVEL 5, GPQA Rein et al. [2024], MUSR Sprague et al. [2024], and MMLU-PRO Wang et al. [2024]. EleutherAI’s Language Model Evaluation Harness Biderman et al. [2024] provides the infrastructure supporting *hundreds* of individual task implementations and has become the backbone for most public leaderboards.

Knowledge and reasoning. MMLU Hendrycks et al. [2021a] tests knowledge across 57 academic subjects via 15,908 questions, and remains the most widely reported single benchmark. MMLU-PRO Wang et al. [2024] extends this with harder multi-step reasoning items. ARC Clark et al. [2018] provides 7,787 grade-school science questions with an easy/challenge split. HELLASWAG Zellers et al. [2019] offers 10,042 commonsense reasoning items, while WINOGRANDE Sakaguchi et al. [2020] contributes 44,000 coreference resolution problems. For mathematics, GSM8K Cobbe et al. [2021] provides 8,500 grade-school word problems and MATH Hendrycks et al. [2021b] targets 12,500 competition-level problems across multiple difficulty levels. BIG-BENCH Srivastava et al. [2023] contributed **204 tasks** from 450 authors across dozens of categories, though in practice only a curated subset (BIG-BENCH HARD) sees regular use. GPQA Rein et al. [2024] adds 448 graduate-level questions in biology, physics, and chemistry.

Code generation. HUMANEVAL Chen et al. [2021] established function-level code evaluation with 164 programming problems. MBPP Austin et al. [2021] provides 974 mostly basic programming tasks. SWE-BENCH Jimenez et al. [2024] raised the bar with 2,294 repository-level tasks drawn from real GitHub issues across 12 Python repositories.

Long-context evaluation. As context windows have grown beyond 100K tokens, benchmarks like RULER Hsieh et al. [2024] with 13 configurable tasks and LONGBENCH Bai et al. [2024] with 21 datasets across 6 task categories have emerged to test whether models can effectively utilize their full context.

Safety and alignment. TRUTHFULQA Lin et al. [2022] provides 817 questions across 38 categories measuring tendency toward factual errors. BBQ Parrish et al. [2022] evaluates social biases across 9 protected categories. HARBENCH Mazeika et al. [2024] standardizes evaluation of 18 red-teaming methods against 33 target models.

Human preference and open-ended evaluation. CHATBOT ARENA Chiang et al. [2024] has accumulated over 240,000 pairwise human votes to produce Elo-style rankings that capture conversational quality static benchmarks miss. MT-BENCH Zheng et al. [2023] uses 80 expert-written multi-turn questions with LLM-as-judge evaluation. ALPACAEVAL 2.0 Dubois et al. [2024] provides length-controlled automatic evaluation to approximate human preference at scale.

Benchmark redundancy and selection. A growing body of work has observed that many of these evaluations provide redundant signals. Polo et al. [2024] proposed TINYBENCHMARKS, demonstrating that curated subsets of approximately 100 examples can accurately estimate full benchmark performance, suggesting substantial redundancy *within* individual benchmarks. In follow-up work, Polo et al. [2025] introduced SLOTH (Skills Scaling Laws), showing that low-dimensional latent skills can predict performance *across* benchmark families simultaneously. Perlitz et al. [2024] proposed BENCHBENCH, a meta-benchmark using Benchmark Agreement Testing to evaluate whether benchmarks actually agree on model rankings, finding significant inconsistencies. Biderman et al. [2024] documented widespread reproducibility challenges across evaluation setups.

B Submodularity

B.1 Lazy Greedy Acceleration

The proof of Theorem 1 tracks the greedy gain at each step relative to the remaining gap to the optimum. At step i , submodularity and monotonicity yield $\Delta(v^* | S_{i-1}) \geq \frac{1}{k}(f(S^*) - f(S_{i-1}))$. Writing $\delta_i = f(S^*) - f(S_i)$, this gives $\delta_i \leq (1 - 1/k)\delta_{i-1}$, so $\delta_k \leq (1 - 1/k)^k f(S^*) \leq f(S^*)/e$.

Lazy greedy acceleration. A naïve greedy implementation recomputes the marginal gain $\Delta(v | S_{i-1})$ for every candidate v at every step, requiring $O(nk)$ function evaluations in total. Minoux [1978] observed that most of these evaluations are wasted: submodularity guarantees that marginal gains can only decrease as the selected set grows, so the gain computed at an earlier step remains a valid *upper bound* on the current gain.

The lazy greedy algorithm exploits this by maintaining a max-heap keyed on the most recently computed marginal gains. At each step, it pops the top element v from the heap and recomputes its true marginal gain $\Delta(v | S_{i-1})$. If the recomputed value is still at least as large as the key of the next element in the heap, then v is the greedy choice and is added to S . Otherwise, v is reinserted into the heap with its updated gain and the process repeats. Each element’s gain is recomputed only when it reaches the top of the heap, and elements whose gains were already small are rarely re-evaluated. In practice, this reduces the total number of function evaluations from $O(nk)$ to nearly $O(n + k \log n)$, with the exact savings depending on the curvature of f .

B.2 Budgeted Maximization

When elements have non-uniform costs $c(v)$, the cardinality constraint is replaced by a budget constraint:

$$\max_{S \subseteq \mathcal{V}} f(S) \quad \text{subject to} \quad c(S) = \sum_{v \in S} c(v) \leq \mathcal{C}. \quad (10)$$

Standard greedy can perform arbitrarily badly in this setting: a single expensive element may consume the entire budget while providing little value. Krause and Guestrin [2005] propose a modified greedy algorithm that runs two strategies in parallel. The first is a *cost-effective greedy*: at each step, select the affordable element with the largest ratio of marginal gain to cost, $\Delta(v | S)/c(v)$, and continue until the budget is exhausted. The second is a *best-singleton strategy*: simply pick the single element with the highest f -value that fits within the budget. The algorithm returns whichever of the two solutions achieves higher objective value.

Theorem 3 (Krause and Guestrin [2005]) *Let f be monotone submodular with $f(\emptyset) = 0$, and let S^* be optimal for (10). The modified greedy returns A with:*

$$f(A) \geq \frac{1}{2}(1 - 1/e) \cdot f(S^*) \approx 0.316 \cdot f(S^*).$$

Sviridenko [2004] showed that partial enumeration of triples followed by greedy fill recovers the full $(1 - 1/e)$ guarantee under knapsack constraints, at $O(n^5)$ cost. Mirzasoleiman et al. [2015] introduced stochastic greedy, achieving $(1 - 1/e - \varepsilon)$ with $O(n \log(1/\varepsilon))$ evaluations per step. For benchmark selection with n in the hundreds, the simpler modified greedy of Krause and Guestrin [2005] suffices.

B.3 Budget Constraint for Entropy

When benchmarks have non-uniform costs $c_j > 0$, the cardinality constraint is replaced by $\sum_{j \in \mathcal{A}} c_j \leq \mathcal{C}$. Following Krause and Guestrin [2005], two strategies are run in parallel: a cost-effective greedy that selects the affordable element with the largest gain-to-cost ratio $\Delta_c(j | \mathcal{A})/c_j$ until the budget is exhausted, and a best-singleton strategy that picks the single most informative benchmark within budget. Here $\Delta_c(j | \mathcal{A}) = \frac{1}{2} \log(2\pi e d_j) + c$ is the shifted entropy marginal, with c chosen so that these marginals are non-negative over the range of subsets considered. As such, the change relative to 1 is minimal. Replace $j^* \leftarrow \operatorname{argmax}_{j \in \mathcal{V} \setminus \mathcal{A}} d_j$ by $j^* \leftarrow \operatorname{argmax}_{j \in \mathcal{V} \setminus \mathcal{A}} \Delta_c(j | \mathcal{A})/c_j$. The best singleton is found in the same shifted objective among benchmarks with $c_j \leq \mathcal{C}$. Subsequently we pick which one of the two solutions (singleton vs. set) is better.

C Numerical Details

The proof of Theorem 2(a) relies on the fact that the marginal gain of adding v to S is $\Delta(v | S) = H(X_v | X_S) = \frac{1}{2} \log(2\pi e \cdot \sigma_{v|S}^2)$, where $\sigma_{v|S}^2$ is the conditional variance. Since conditioning on more variables can

only reduce variance, $\sigma_{v|S}^2 \geq \sigma_{v|T}^2$ whenever $S \subseteq T$, giving submodularity. Krause et al. [2008] extended this framework to robust objectives and matroid constraints.

For (b), the MI expansion (8) and the marginal gain (9) are derived in the main text (Section 3). Submodularity follows because $\sigma_{v|S}^2$ is non-increasing in S while $\sigma_{v|\mathcal{V} \setminus (S \cup \{v\})}^2$ is non-decreasing. Unlike entropy, mutual information is *not* monotone: once S covers most of the information about $\mathcal{V} \setminus S$, adding elements shrinks the set being predicted, decreasing f_2 .

Both conditional variances have closed forms via the Schur complement:

$$\sigma_{v|S}^2 = \Sigma_{vv} - \Sigma_{vS} \Sigma_{SS}^{-1} \Sigma_{Sv}, \quad (11)$$

$$\sigma_{v|\bar{S}_v}^2 = \Sigma_{vv} - \Sigma_{v\bar{S}_v} \Sigma_{\bar{S}_v\bar{S}_v}^{-1} \Sigma_{\bar{S}_v v}. \quad (12)$$

For the entropy objective f_1 , only (11) is needed. Since the greedy algorithm *grows* S one element at a time, we can maintain a Cholesky factorization of Σ_{SS} via rank-one updates at cost $O(k^2n)$ overall.

For the mutual information objective f_2 , both quantities enter through (9). The difficulty with (12) is that the conditioning set \bar{S}_v *shrinks* as S grows, so incremental Cholesky updates, which add columns, do not apply. We use the identity $\sigma_{v|\bar{S}_v}^{-2} = [(\Sigma_{\bar{S},\bar{S}})^{-1}]_{vv}$, where $\bar{S} = \mathcal{V} \setminus S$ is the complement [Golub and Van Loan, 2013, §4.2].

Rank One Modifications A natural approach is to precompute $P = \Sigma_{\mathcal{V}}^{-1}$ and maintain P restricted to $\mathcal{V} \setminus S$ via rank-one downdates: when element j is selected, update

$$P_{ab} \leftarrow P_{ab} - (P_{aj} P_{jb}) / P_{jj} \quad a, b \in \mathcal{V} \setminus (S \cup \{j\}) \quad (13)$$

at cost $O(n^2)$ per step. However, this is numerically unstable: when P_{jj} is small (i.e. benchmark j has large conditional variance given the complement), the division amplifies rounding errors, and iterated downdates accumulate these errors across steps. Simply adding a ridge term λI to Σ before inversion perturbs the mutual information values themselves, which is undesirable.

Instead, we recompute P_{vv} from a *fresh* Cholesky factorization of the complement block at each step. While this increases the order of the computation, the practical overhead is negligible if we have only hundreds of benchmarks. Writing $L_{\bar{S}} L_{\bar{S}}^\top = \Sigma_{\bar{S},\bar{S}}$, the precision diagonal is

$$P_{vv} = \|(L_{\bar{S}}^{-1})_{:,v}\|^2, \quad v \in \bar{S}, \quad (14)$$

obtained by a single triangular solve $L_{\bar{S}}^{-1}$ at cost $O(|\bar{S}|^3)$. When the complement block is near-singular (as in rank-deficient settings with $M < N$), we fall back to an eigendecomposition $\Sigma_{\bar{S},\bar{S}} = V \Lambda V^\top$ with clamped eigenvalues, giving $P_{vv} = \sum_j V_{vj}^2 / \lambda_j$. This eliminates all accumulated roundoff from iterated downdates. For moderate n (hundreds of benchmarks), the constant-factor overhead of refactorization is negligible.

Cost Analysis The dominant cost of Algorithm 2 is the complement refactorization at $O(|\bar{\mathcal{A}}|^3) = O(N^3)$ per step; the Cholesky update adds $O(tN)$. Over k steps the total is $O(kN^3)$, one extra factor of N compared with the $O(kN^2)$ rank-one downdate (13), but for N in the hundreds and $k \leq 15$ the wall-clock overhead is negligible (under one second on all our datasets). Lazy evaluation applies to the selection criterion but not to the refactorization, which must be performed eagerly.

D Dataset Details

We assemble score matrices from ten public leaderboards spanning general language understanding, code generation, embedding quality, instruction following, and safety. Table 1 summarizes the retained dimensions for the experiment matrices. Together they provide a diverse testbed for benchmark selection: the number of tasks per collection ranges from 1 to 57, and missingness fractions vary from 0% to 22.7%.

General-purpose leaderboards. The OPEN LLM LEADERBOARD v2 [Open LLM Leaderboard Team, 2024] reports scores on six benchmarks (IFEVAL, BBH, MATH LVL5, GPQA, MUSR, MMLU-PRO) for thousands of open-weight models. HELM LITE [Liang et al., 2023] provides holistic evaluation across approximately ten core scenarios covering summarisation, question answering, and knowledge tasks. MMLU [Hendrycks et al., 2021a] partitions knowledge evaluation into 57 academic subjects, yielding a wide per-subject score matrix that is ideal for studying benchmark redundancy.

Table 1: Summary of benchmark collections. M = number of models, N = number of tasks or sub-benchmarks retained for the experiments, and % miss. denotes the fraction of missing entries in the score matrix.

| Dataset | M | N | % miss. |
|--------------------|-------|-----|---------|
| MMLU (per-subject) | 5 452 | 57 | 0.0 |
| OPEN LLM v2 | 4 507 | 6 | 0.1 |
| MTEB | 263 | 56 | 22.7 |
| ALPACAEVAL 2 | 223 | 3 | 0.0 |
| LIVEBENCH | 195 | 3 | 11.3 |
| BIGCODEBENCH | 155 | 14 | 10.0 |
| WILDBENCH | 63 | 11 | 0.0 |
| ARENA-HARD | 60 | 1 | 0.0 |
| HELM LITE | 30 | 11 | 0.0 |
| MT-BENCH | 5 | 8 | 0.0 |

Instruction-following and chat evaluation. ALPACAEVAL 2 [Dubois et al., 2024] computes length-controlled win-rates against a reference model using GPT-4-Turbo as judge. MT-BENCH [Zheng et al., 2023] evaluates multi-turn dialogue quality across eight categories (writing, roleplay, reasoning, math, coding, extraction, STEM, humanities) with GPT-4 scoring each response on a 1–10 scale. ARENA-HARD-AUTO [Li et al., 2024] benchmarks models on 500 challenging user prompts derived from CHATBOT ARENA, reporting automated judge scores. LIVEBENCH [White et al., 2025] provides a continuously refreshed set of tasks across six categories (math, coding, reasoning, language, data analysis, instruction following), mitigating contamination. WILDBENCH [Lin et al., 2024] collects real user queries and evaluates models with per-category score breakdowns.

Embedding and code benchmarks. MTEB [Muennighoff et al., 2023] evaluates text embedding models on 56 English tasks spanning retrieval, classification, clustering, and semantic similarity. BIGCODEBENCH [Zhuo et al., 2025] measures code generation performance on tasks derived from HUMANEVAL [Chen et al., 2021] and MBPP [Austin et al., 2021], including hardened variants.

We omit BIG-BENCH LITE [Srivastava et al., 2023] as its 55 models are internal Google checkpoints that do not appear in any other collection, precluding cross-benchmark analysis.

Experiment matrices. From the ten collections above we construct three score matrices for our experiments. MMLU ($5\,452 \times 57$, fully observed) provides a large, dense matrix of per-subject knowledge scores. Two models with fewer than half their entries observed were dropped. MTEB (263×56 , 77.3% observed) covers embedding models across diverse retrieval and similarity tasks, with moderate missingness. Five models with only a single observed benchmark were dropped, as they contribute no pairwise covariance information. MERGED (118×114 , 31.1% observed) combines all collections except MTEB by canonicalizing model names across leaderboards (Appendix E): rows are the 118 models that appear in at least two collections, and columns are collection-prefixed task names, yielding a heterogeneous, sparse matrix that exercises the missing-data machinery of Section 3. Auxiliary count, uncertainty, and length columns are excluded so that all columns represent benchmark scores or win rates.

E Model Canonicalization

To merge score matrices from different benchmark collections into a unified table, we must identify when the same model appears under different names. Table 2 lists the 118 models that we identified across at least two collections. Column headers abbreviate the benchmark names: OL2 = OPEN LLM v2, HELM = HELM LITE, AE2 = ALPACAEVAL 2, AH = ARENA-HARD, LB = LIVEBENCH, WB = WILDBENCH, MT = MT-BENCH, BC = BIGCODEBENCH. Table 3 lists models that could not be matched to any other collection; the per-collection details are in Section E.1. Figure 8 visualizes the pairwise overlap: nodes represent benchmark collections (colored by category, numbered by canonical models matched), and edge widths are proportional to the number of shared models. The instruction-following and chat benchmarks form a densely connected core.

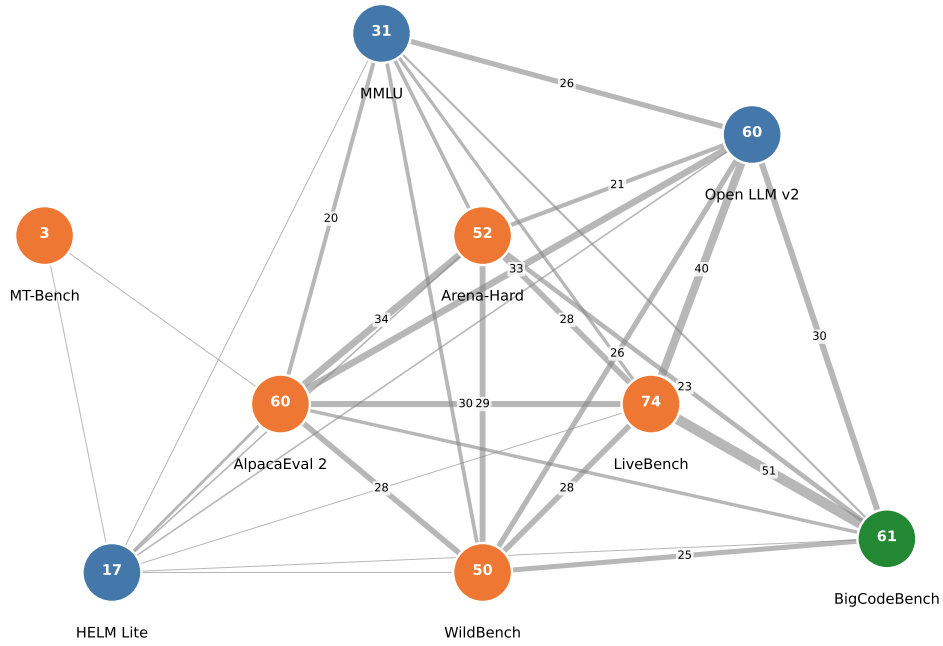
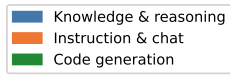


Figure 8: Benchmark overlap network. Each node is a collection; the number inside shows how many of the 118 canonical models appear in it. Edge width is proportional to the number of shared models; labels show counts ≥ 20 . MTEB is omitted as its embedding models have no overlap with any other collection.

Table 2: Canonical model mapping across benchmark collections. A check mark indicates that the model is present in the corresponding collection. Models are sorted by the number of collections in which they appear.

| Model | MMLU | OL2 | HELM | AE2 | AH | LB | WB | MT | BC | MTEB | n |
|-----------------------------|------|-----|------|-----|----|----|----|----|----|------|-----|
| Meta-Llama-3-70B-Instruct | ✓ | ✓ | | ✓ | ✓ | ✓ | ✓ | | ✓ | | 7 |
| Meta-Llama-3-8B-Instruct | ✓ | ✓ | | ✓ | ✓ | ✓ | ✓ | | ✓ | | 7 |
| Mixtral-8x7B-Instruct-v0.1 | ✓ | ✓ | ✓ | ✓ | ✓ | ✓ | ✓ | | | | 7 |
| Mixtral-8x22B-Instruct-v0.1 | ✓ | ✓ | | ✓ | ✓ | ✓ | | | ✓ | | 6 |
| Phi-3-mini-128k-instruct | ✓ | ✓ | | | ✓ | ✓ | ✓ | | ✓ | | 6 |
| Qwen1.5-72B-Chat | ✓ | | | ✓ | ✓ | ✓ | ✓ | | ✓ | | 6 |
| Qwen2-72B-Instruct | | ✓ | | ✓ | ✓ | ✓ | ✓ | | ✓ | | 6 |
| claude-3-5-sonnet-20240620 | | | | ✓ | ✓ | ✓ | ✓ | | ✓ | | 5 |
| claude-3-opus-20240229 | | | | ✓ | ✓ | ✓ | ✓ | | ✓ | | 5 |
| claude-3-sonnet-20240229 | | | | ✓ | ✓ | ✓ | ✓ | | ✓ | | 5 |
| command-r-plus | ✓ | ✓ | | | ✓ | | ✓ | | ✓ | | 5 |
| gemma-2-27b-it | | ✓ | | | ✓ | ✓ | ✓ | | ✓ | | 5 |
| gemma-2b-it | ✓ | ✓ | | ✓ | ✓ | | ✓ | | | | 5 |
| gemma-7b-it | ✓ | ✓ | | ✓ | ✓ | | ✓ | | | | 5 |
| gpt-4-0613 | | | ✓ | ✓ | ✓ | ✓ | | | ✓ | | 5 |
| gpt-4-turbo-2024-04-09 | | | | ✓ | ✓ | ✓ | ✓ | | ✓ | | 5 |

continued on next page

| Model | MMLU | OL2 | HELM | AE2 | AH | LB | WB | MT | BC | MTEB | n |
|---------------------------------|------|-----|------|-----|----|----|----|----|----|------|---|
| gpt-4o-2024-05-13 | | | | ✓ | ✓ | ✓ | ✓ | | ✓ | | 5 |
| gpt-4o-mini-2024-07-18 | | | | ✓ | ✓ | ✓ | ✓ | | ✓ | | 5 |
| llama-2-70b | | ✓ | ✓ | ✓ | ✓ | ✓ | ✓ | | | | 5 |
| llama-2-7b | | ✓ | ✓ | ✓ | ✓ | ✓ | ✓ | | | | 5 |
| Meta-Llama-3.1-70B-Instruct | | ✓ | | ✓ | ✓ | ✓ | | | ✓ | | 5 |
| Meta-Llama-3.1-8B-Instruct | | ✓ | | ✓ | ✓ | ✓ | | | ✓ | | 5 |
| Mistral-7B-Instruct-v0.2 | ✓ | ✓ | | ✓ | | ✓ | ✓ | | | | 5 |
| mistral-large-2402 | | | | ✓ | ✓ | ✓ | ✓ | | ✓ | | 5 |
| Phi-3-medium-128k-instruct | ✓ | ✓ | | | | ✓ | ✓ | | ✓ | | 5 |
| Qwen1.5-110B-Chat | ✓ | ✓ | | ✓ | | ✓ | | | ✓ | | 5 |
| Qwen1.5-7B-Chat | ✓ | ✓ | | ✓ | | ✓ | ✓ | | | | 5 |
| yi-34b | ✓ | ✓ | ✓ | ✓ | ✓ | | | | | | 5 |
| claude-3-haiku-20240307 | | | | | ✓ | ✓ | ✓ | | ✓ | | 4 |
| command-r | ✓ | ✓ | | | ✓ | | ✓ | | | | 4 |
| dbrx-instruct | ✓ | ✓ | | ✓ | | | ✓ | | | | 4 |
| falcon-40b | ✓ | ✓ | ✓ | ✓ | | | | | | | 4 |
| gemma-1.1-7b-it | ✓ | ✓ | | | ✓ | ✓ | | | | | 4 |
| gemma-2-9b-it | | ✓ | | | | ✓ | ✓ | | ✓ | | 4 |
| gpt-3.5-turbo-0125 | | | | | ✓ | ✓ | ✓ | | ✓ | | 4 |
| Llama-2-70b-chat-hf | | ✓ | | ✓ | ✓ | ✓ | ✓ | | | | 4 |
| Llama-2-7b-chat-hf | | ✓ | | ✓ | | ✓ | ✓ | | | | 4 |
| Mistral-7B-Instruct-v0.3 | | ✓ | | ✓ | | ✓ | | | ✓ | | 4 |
| OpenHermes-2.5-Mistral-7B | ✓ | ✓ | | ✓ | | ✓ | | | | | 4 |
| Phi-3-medium-4k-instruct | ✓ | ✓ | | | ✓ | ✓ | | | | | 4 |
| Qwen1.5-1.8B-Chat | ✓ | ✓ | | ✓ | | ✓ | | | | | 4 |
| Starling-LM-7B-alpha | ✓ | ✓ | | ✓ | ✓ | | | | | | 4 |
| Starling-LM-7B-beta | ✓ | | | | ✓ | ✓ | ✓ | | | | 4 |
| tulu-2-dpo-70b | ✓ | | | ✓ | ✓ | | ✓ | | | | 4 |
| yi-1.5-34b-chat | ✓ | ✓ | | | | | ✓ | | ✓ | | 4 |
| yi-1.5-6b-chat | ✓ | ✓ | | | | | ✓ | | ✓ | | 4 |
| yi-1.5-9b-chat | ✓ | ✓ | | | | | ✓ | | ✓ | | 4 |
| Yi-34B-Chat | ✓ | ✓ | | ✓ | ✓ | | | | | | 4 |
| yi-6b | ✓ | ✓ | ✓ | | | ✓ | | | | | 4 |
| claude-2.1 | | | ✓ | ✓ | ✓ | | | | | | 3 |
| Claude-v1 | | | ✓ | ✓ | | | | ✓ | | | 3 |
| command-r-08-2024 | | ✓ | | | | ✓ | | | ✓ | | 3 |
| deepseek-r1-distill-llama-70b | | ✓ | | | | ✓ | | | ✓ | | 3 |
| deepseek-r1-distill-qwen-32b | | ✓ | | | | ✓ | | | ✓ | | 3 |
| falcon-7b | | ✓ | ✓ | ✓ | | | | | | | 3 |
| gemma-2-9b-it-DPO | | ✓ | | ✓ | | | ✓ | | | | 3 |
| gemma-2-9b-it-SimPO | | ✓ | | ✓ | | | ✓ | | | | 3 |
| gpt-3.5-turbo-0613 | | | ✓ | ✓ | ✓ | | | | | | 3 |
| gpt-3.5-turbo-1106 | | | | ✓ | ✓ | ✓ | | | | | 3 |
| gpt-4-0125-preview | | | | | ✓ | ✓ | ✓ | | | | 3 |
| gpt-4-1106-preview | | | ✓ | ✓ | | ✓ | | | | | 3 |
| llama-2-13b | | ✓ | ✓ | ✓ | | ✓ | | | | | 3 |
| Llama-3-Instruct-8B-SimPO | | ✓ | | ✓ | | | ✓ | | | | 3 |
| Llama-3-Instruct-8B-SimPO-ExPO | | ✓ | | ✓ | | | ✓ | | | | 3 |
| llama-3.1-nemotron-70b-instruct | | ✓ | | | | ✓ | | | ✓ | | 3 |
| llama-3.3-70b-instruct | | ✓ | | | | ✓ | | | ✓ | | 3 |
| Meta-Llama-3.1-405B-Instruct | | | | ✓ | ✓ | ✓ | | | | | 3 |
| mistral-large-2407 | | | | | ✓ | ✓ | ✓ | | | | 3 |
| mistral-small-2409 | | ✓ | | | | ✓ | | | ✓ | | 3 |

continued on next page

| Model | MMLU | OL2 | HELM | AE2 | AH | LB | WB | MT | BC | MTEB | n |
|---------------------------------|------|-----|------|-----|----|----|----|----|----|------|---|
| phi-3-small-128k-instruct | | ✓ | | | | ✓ | | | ✓ | | 3 |
| Phi-3-small-8k-instruct | | ✓ | | | ✓ | ✓ | | | | | 3 |
| phi-3.5-mini-instruct | | ✓ | | | | ✓ | | | ✓ | | 3 |
| phi-4 | | ✓ | | | | ✓ | | | ✓ | | 3 |
| qwen2-7b-instruct | | ✓ | | | | ✓ | | | ✓ | | 3 |
| qwen2.5-72b-instruct | | ✓ | | | | ✓ | | | ✓ | | 3 |
| qwen2.5-7b-instruct | | ✓ | | | | ✓ | | | ✓ | | 3 |
| qwen2.5-coder-32b-instruct | | ✓ | | | | ✓ | | | ✓ | | 3 |
| qwq-32b-preview | | ✓ | | | | ✓ | | | ✓ | | 3 |
| Snorkel-Mistral-PairRM-DPO | ✓ | | | ✓ | ✓ | | | | | | 3 |
| Starling-LM-7B-beta-ExPO | ✓ | | | ✓ | | | ✓ | | | | 3 |
| vicuna-7b-v1.5 | | ✓ | | ✓ | | ✓ | | | | | 3 |
| yi-large | | | | | ✓ | | ✓ | | ✓ | | 3 |
| yi-large-preview | | | | ✓ | ✓ | | ✓ | | | | 3 |
| zephyr-7b-alpha | | ✓ | | ✓ | | ✓ | | | | | 3 |
| zephyr-7b-beta | | ✓ | | ✓ | | ✓ | | | | | 3 |
| athene-70b | | | | | | | ✓ | | ✓ | | 2 |
| claude-2.0 | | | ✓ | | ✓ | | | | | | 2 |
| claude-3-5-haiku-20241022 | | | | | | ✓ | | | ✓ | | 2 |
| claude-3-5-sonnet-20241022 | | | | | | ✓ | | | ✓ | | 2 |
| claude-instant-1.2 | | | ✓ | ✓ | | | | | | | 2 |
| Cohere-Command | | | ✓ | ✓ | | | | | | | 2 |
| deepseek-coder-v2 | | | | | ✓ | | ✓ | | | | 2 |
| deepseek-coder-v2-lite-instruct | | | | | | ✓ | | | ✓ | | 2 |
| DeepSeek-V2-Chat | | | | | | | ✓ | | ✓ | | 2 |
| DeepSeek-V2-Chat-0628 | | | | | | | ✓ | | ✓ | | 2 |
| deepseek-v3 | | | | | | ✓ | | | ✓ | | 2 |
| Gemini-1.5-Flash | | | | | | ✓ | ✓ | | | | 2 |
| gemini-1.5-flash-api-0514 | | | | | ✓ | | | | ✓ | | 2 |
| Gemini-1.5-Pro | | | | | | ✓ | ✓ | | | | 2 |
| gemini-1.5-pro-api-0514 | | | | | ✓ | | | | ✓ | | 2 |
| gemini-2.0-flash-exp | | | | | | ✓ | | | ✓ | | 2 |
| gemini-exp-1114 | | | | | | ✓ | | | ✓ | | 2 |
| gemini-exp-1121 | | | | | | ✓ | | | ✓ | | 2 |
| gemini-exp-1206 | | | | | | ✓ | | | ✓ | | 2 |
| gemini-pro | | | | ✓ | ✓ | | | | | | 2 |
| GPT-3.5-Turbo | | | | ✓ | | | | ✓ | | | 2 |
| GPT-4 | | | | ✓ | | | | ✓ | | | 2 |
| gpt-4-0314 | | | | ✓ | ✓ | | | | | | 2 |
| gpt-4o-2024-11-20 | | | | | | ✓ | | | ✓ | | 2 |
| llama-4-maverick | | | | | | ✓ | | | ✓ | | 2 |
| Mistral-7B-Instruct-v0.1 | | | ✓ | | ✓ | | | | | | 2 |
| mistral-medium | | | ✓ | ✓ | | | | | | | 2 |
| Mistral-Nemo-Instruct-2407 | | | | | | ✓ | ✓ | | | | 2 |
| mistral-small-2402 | | | | | | ✓ | | | ✓ | | 2 |
| mistral-small-2501 | | | | | | ✓ | | | ✓ | | 2 |
| Phi-3-Mini-128K-Instruct | | | | | | ✓ | | | ✓ | | 2 |
| sky-t1-32b-preview | | | | | | ✓ | | | ✓ | | 2 |
| Vicuna-33B-v1.3 | | | | ✓ | ✓ | | | | | | 2 |

E.1 Unmatched Models by Collection

MMLU 5,424 of 5,454 models unmatched (not listed).

Open LLM v2 4,450 of 4,507 models unmatched (not listed).

HELM Lite (13 of 30 unmatched)

Cohere Command Light, GPT-3.5 (text-davinci-002), GPT-3.5 (text-davinci-003), Jurassic-2 Grande (17B), Jurassic-2 Jumbo (178B), LLaMA (65B), Luminous Base (13B), Luminous Extended (30B), Luminous Supreme (70B), PaLM-2 (Bison), PaLM-2 (Unicorn), Palmyra X V2 (33B), Palmyra X V3 (72B)

AlpacaEval 2 166 of 223 models unmatched (not listed).

Arena-Hard (10 of 60 unmatched)

athene-70b-0725, dbrx-instruct-preview, gemini-1.5-pro-api-0409-preview, gemma-1.1-2b-it, glm-4-0116, glm-4-0520, glm-4-air, gpt-3.5-turbo-0314, mistral-next, snowflake-arctic-instruct

LiveBench 121 of 195 models unmatched (not listed).

WildBench (15 of 63 unmatched)

Hermes-2-Theta-Llama-3-8B, Llama-3-8B-Magpie-Align-v0.1, Llama-3-Instruct-8B-SimPO-v0.2, Nous-Hermes-2-Mixtral-8x7B-DPO, SELM-Llama-3-8B-Instruct-iter-3, SELM-Zephyr-7B-iter-3, deepseek-v2-coder-0628, gemma-2-2b-it, glm-4-9b-chat, nemotron-4-340b-instruct, neo_7b_instruct_v0.1, neo_7b_instruct_v0.1-ExPO, reka-core-20240501, reka-edge, reka-flash-20240226

MT-Bench (2 of 5 unmatched)

alpaca-13b, llama-13b

BigCodeBench 94 of 155 models unmatched (not listed).

MTEB 268 of 268 models unmatched (not listed).

F Selection Order and Stability

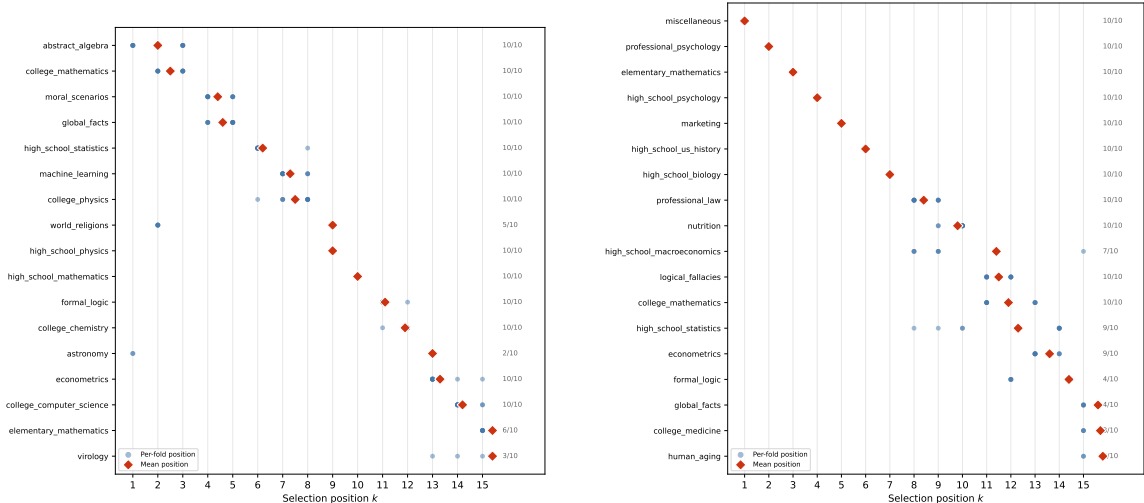
Beyond imputation quality, it is important to examine *which* benchmarks the greedy algorithm selects, and how stable this selection is across folds. Figures 9–11 show, for the 10% holdout (maximum training data), the selection position of each benchmark across the 10 folds. Blue dots indicate individual fold positions; red diamonds mark the mean; the right margin shows how many folds (out of 10) include each benchmark in their top-15.

MMLU selection is exceptionally stable (Figure 9a). The top two benchmarks are `abstract_algebra` and `college_mathematics` (both 10/10 folds, mean positions 2.2 and 2.4), followed by `moral_scenarios` and `global_facts` (both 10/10, mean position 4.5). The first position rotates: `abstract_algebra` takes it in 4/10 folds, with `business_ethics`, `college_chemistry`, `astronomy`, and others occasionally claiming it, but these alternatives always appear later in the remaining folds. Of the top 15 benchmarks, the majority appear in all 10 folds; only `world_religions` (5/10) and `business_ethics` (2/10) show meaningful instability. The tight clustering of per-fold dots confirms that the dominant correlation structure of MMLU is robustly estimated.

Interestingly, the greedy algorithm favors subjects that are intuitively “different” from one another: `abstract_algebra` (formal reasoning), `college_mathematics` (quantitative), `moral_scenarios` (ethical judgment), `global_facts` (world knowledge), `high_school_statistics` (data literacy), `machine_learning` (technical). This diversity is not imposed; it emerges naturally from entropy maximization, which penalizes redundancy among selected benchmarks.

MTEB. Figure 10a shows moderate stability. `SummEval` is always selected second (10/10, mean position 2.0), serving as a strong anchor for summarization evaluation. `MTOPDomainClassification` and `AmazonCounterfactualClassification` are both selected in all 10 folds (mean positions 4.3). The next tier (`STS17` at 9/10, `Touche2020` at 9/10) appears in most folds but with more positional spread; the first position rotates among diverse benchmarks. The selected set spans the major MTEB task categories: semantic textual similarity (`STS12`, `STS17`, `STS22`), classification (`AmazonCounterfactualClassification`, `ToxicConversationsClassification`), clustering (`StackExchangeClusteringP2P`), reranking (`MindSmallReranking`), and retrieval (`SCIDOCS`). Again, this category diversity emerges from the entropy objective without explicit category-awareness.

MERGED selection is highly unstable (Figure 11a), with most benchmarks appearing in only 2–5 out of 10 folds. The most consistent entropy selections are OPEN LLM’s `MUSR` (10/10), `bigcode/Network_complete`



(a) Entropy selection. Nearly all benchmarks appear in all 10 folds at nearly identical positions, indicating highly stable selection.

(b) MI selection. The first 9 benchmarks are identical across all 10 folds, starting with miscellaneous, a high-connectivity hub subject.

Figure 9: Selection order for MMLU (10% holdout). Entropy (left) selects high-variance “outlier” subjects; MI (right) selects “hub” subjects with strong predictive links to the rest.

(9/10), and helm/NarrativeQA (8/10), while the first position rotates among MMLU, HELM, MT-BENCH, and code benchmarks. This instability is a direct consequence of sparse, heterogeneous data: when off-diagonal correlations are noisy and many benchmarks have similar conditional variance, greedy selection becomes sensitive to minor perturbations in the training set. Despite this instability in the selection *order*, the imputation *quality* (Figure 4) still improves with k , confirming that the overall subspace captured matters more than the specific pivot sequence.

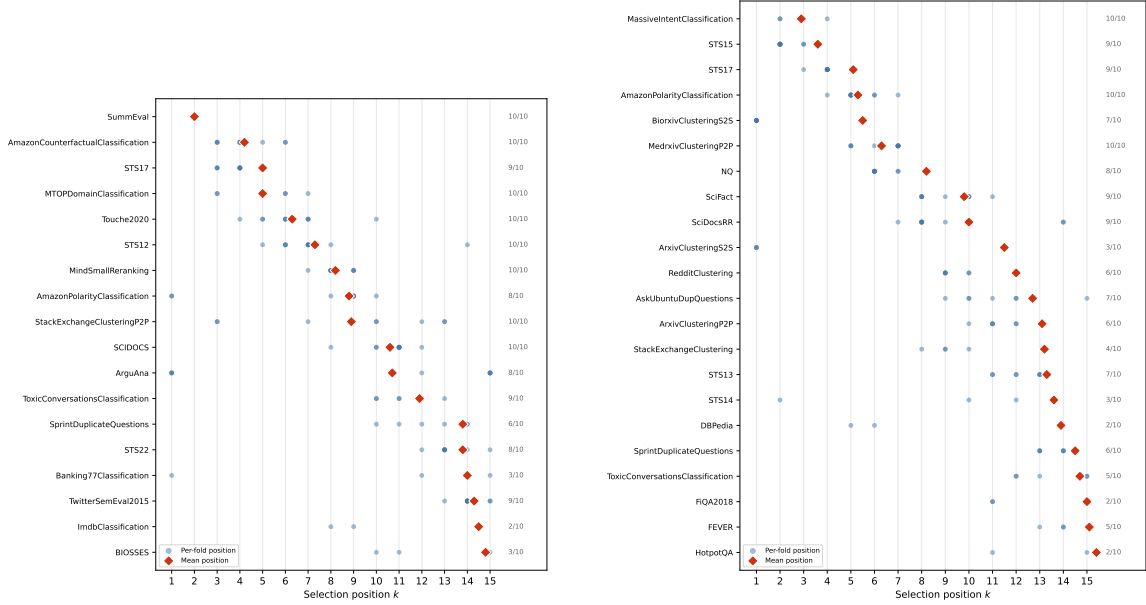
MI selection order. On MMLU (Figure 9b), the first benchmark selected is always miscellaneous (10/10 folds), a broad, multi-topic subject that correlates strongly with many other MMLU tasks. This contrasts sharply with the entropy selection, which begins with abstract_algebra or similar high-variance niche subjects. The next four MI selections (professional_psychology, elementary_mathematics, high_school_psychology, marketing) are equally stable and cover the major capability clusters: quantitative reasoning, social science, and applied knowledge. The selection is remarkably stable, with the first 9 benchmarks appearing in all 10 folds. MI favors “hub” subjects that sit at the center of the correlation network, rather than “outlier” subjects with high marginal variance but limited predictive power for the rest.

On MTEB (Figure 10b), MassiveIntentClassification (10/10, mean rank 2.9) emerges as the top MI pick, an intent-classification task that spans many semantic categories and thus serves as a strong predictor for the rest. The next selections include STS15 (9/10), STS17 (9/10), and AmazonPolarityClassification (10/10), covering semantic similarity and sentiment.

On the MERGED dataset (Figure 11b), MI consistently selects arena_hard/score first in all 10 folds, with helm/NarrativeQA (8/10), open_llm/MUSR (8/10), and open_llm/IFEval (7/10) appearing frequently later. The selection is notably less stable than on MMLU or MTEB, reflecting the challenging sparse estimation regime (31.1% observed). Nevertheless, MI reliably picks benchmarks from diverse evaluation families (chat, knowledge, code), consistent with its objective of maximizing predictive coverage of the complement.

G EM Algorithm for Covariance Estimation

We give the full EM update equations for estimating (μ, Σ) from an incomplete score matrix $B \in \mathbb{R}^{M \times N}$ with observation mask $O \in \{0, 1\}^{M \times N}$.



(a) Entropy selection. SummEval is consistently selected second (10/10); MTOPDomainClassification and AmazonCounterfactualClassification anchor the top 5.

(b) MI selection. MassiveIntentClassification is the most stable top pick (10/10, mean rank 2.9), followed by STS15 and STS17.

Figure 10: Selection order for **MTEB** (10% holdout). Entropy (left) leads with high-variance classification tasks; MI (right) leads with the broadly connected MassiveIntentClassification.

Initialization. Set $\mu_j^{(0)} = \hat{\mu}_j$ from (15). For the initial covariance, compute the pairwise-complete estimate (16) and project onto the positive semidefinite cone: eigendecompose, clamp negative eigenvalues to a small $\varepsilon > 0$, and reconstruct. This ensures $\Sigma^{(0)} \succ 0$.

For the per-benchmark mean with missing data, we have

$$\hat{\mu} = B^\top \mathbf{1}_M \oslash O^\top \mathbf{1}_M, \quad (15)$$

where \oslash denotes elementwise division. The pairwise-complete covariance estimate is

$$\hat{\Sigma}^{\text{pw}} = \bar{B}^\top \bar{B} \oslash \max\{O^\top O - \mathbf{1}_N \mathbf{1}_N^\top, \mathbf{1}_N \mathbf{1}_N^\top\}, \quad (16)$$

where $\bar{B}_{ij} = O_{ij}(B_{ij} - \hat{\mu}_j)$ and the maximum is elementwise. The denominator floor avoids division by zero when two benchmarks have only one co-observed model. Note that $\hat{\Sigma}^{\text{pw}}$ is not guaranteed to be positive semidefinite, since each entry is estimated from a different subset of models.

E-step. For each model i , use the current parameters $(\mu^{(t)}, \Sigma^{(t)})$ to compute the conditional moments of the missing benchmarks \bar{B}_i given the observed benchmarks B_i :

$$\mathbb{E}[B_{i,\bar{B}_i} | B_{i,B_i}] = \mu_{\bar{B}_i}^{(t)} + \Sigma_{\bar{B}_i, B_i}^{(t)} (\Sigma_{B_i, B_i}^{(t)})^{-1} (B_{i,B_i} - \mu_{B_i}^{(t)}), \quad (17)$$

$$C_i^{(t)} := \text{Cov}(B_{i,\bar{B}_i} | B_{i,B_i}) = \Sigma_{\bar{B}_i, \bar{B}_i}^{(t)} - \Sigma_{\bar{B}_i, B_i}^{(t)} (\Sigma_{B_i, B_i}^{(t)})^{-1} \Sigma_{B_i, \bar{B}_i}^{(t)}. \quad (18)$$

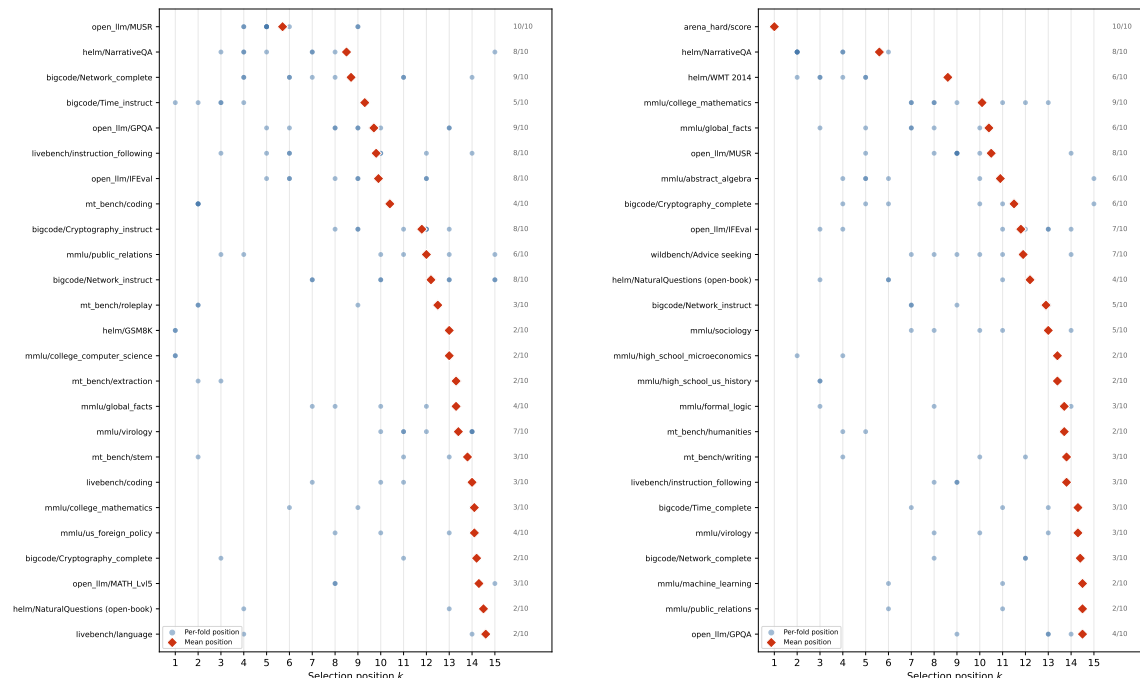
The inversion of $\Sigma_{B_i, B_i}^{(t)}$ is performed via Cholesky factorization. If the submatrix is numerically singular (which can occur in rank-deficient or sparse settings), a small ridge εI is added before factorization.

Let \tilde{B}_i denote the completed row: observed entries are kept, missing entries are filled with their conditional expectations (17).

M-step. Re-estimate μ, Σ from the completed data:

$$\mu^{(t+1)} = \frac{1}{M} \tilde{B}^\top \mathbf{1}_M, \quad (19)$$

$$\Sigma^{(t+1)} = \frac{1}{M} \tilde{B}^\top \tilde{B} + \frac{1}{M} \sum_{i=1}^M C_i^{(t)}, \quad (20)$$



(a) Entropy selection. High instability reflects noisy covariance estimation from sparse data; Open LLM’s MUSR is the only benchmark selected in all 10 folds.

(b) MI selection. arena_hard/score is selected first in all 10 folds, followed by helm/NarrativeQA (8/10). Greater variability reflects the challenging sparse estimation regime.

Figure 11: Selection order for **MERGED** (10% holdout). Both methods show high instability due to sparse data, but MI draws from diverse evaluation families (chat, knowledge, code).

where $\tilde{\tilde{B}} = \tilde{B} - \mathbf{1}_M(\mu^{(t+1)})^\top$ is centered, and $C_i^{(t)}$ is the $N \times N$ matrix whose (j, k) -entry equals (18) when both $j, k \in \tilde{B}_i$, and zero otherwise. This correction term accounts for imputation uncertainty and ensures that $\Sigma^{(t+1)}$ remains positive semidefinite. After each M-step, eigenvalues are clamped to $\varepsilon > 0$ via PSD projection.

Convergence. We monitor both the relative change in Frobenius norm $\|\Sigma^{(t+1)} - \Sigma^{(t)}\|_F / \|\Sigma^{(t)}\|_F$ and the observed-data log-likelihood $\sum_{i=1}^M \log p(B_{i, \tilde{B}_i} | \mu, \Sigma)$. For the fully observed case (MMLU), EM converges in 2–3 iterations. For moderate missingness (MTEB, 23%), convergence takes roughly 300 iterations. For the sparse MERGED matrix (118×114 , 68.9% missing), it converges in 274 iterations.

Rank deficiency and sparsity. When fewer models than benchmarks are available, the empirical completed-data term $\tilde{\tilde{B}}^\top \tilde{\tilde{B}}/M$ in (20) has rank at most $M - 1$; the conditional-covariance correction can increase the rank, but sparse data still produces small, noisy eigenvalues. This causes numerical difficulties in the E-step Cholesky factorizations and prevents the log-likelihood from being a reliable convergence diagnostic (submatrices $\Sigma_{\tilde{B}_i, \tilde{B}_i}$ may become singular). We address rank deficiency with linear shrinkage toward the identity, in the form of Ledoit and Wolf [2004]: $\Sigma^{(0)} \leftarrow (1 - \alpha)\Sigma^{(0)} + \alpha(\text{tr}(\Sigma^{(0)})/N)I$ with the deterministic intensity $\alpha = (N - M)/N$. This ensures all initial eigenvalues are bounded away from zero while preserving the trace, but it also dampens cross-benchmark correlations in data-poor regimes. For either rank-deficient or highly sparse matrices, PSD projection with a floor $\varepsilon = 10^{-3}$ is applied after each M-step, preventing eigenvalue collapse during iteration. After convergence, rank-deficient runs receive the same post-hoc linear shrinkage to ensure the output covariance is well-conditioned for downstream use.

Score normalization. An equally important practical aspect is to standardize each column to (zero mean and) unit variance before computing $\hat{\Sigma}$: a diagonal whitening of the correlation matrix prevents the objective from being dominated by high-variance benchmarks. Obviously this needs to be undone prior to imputation.

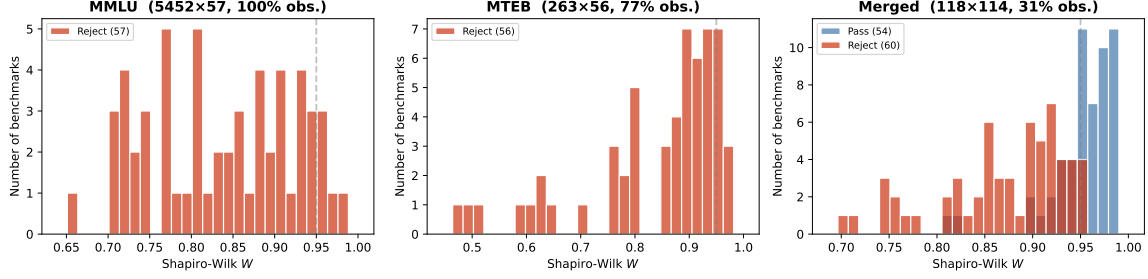


Figure 12: Normality diagnostics: histogram of per-benchmark Shapiro–Wilk W statistics (BH-corrected at $\alpha = 0.05$). All 57 MMLU and 56 MTEB benchmarks reject; on MERGED, 60 of 114 reject (smaller per-benchmark sample sizes reduce power).

H Normality Diagnostics

The Gaussian model is an assumption that should be validated. Leave-one-model-out cross-validation holds out model i , estimates Σ from the rest, selects \mathcal{A} , imputes $\hat{B}_{i,\bar{\mathcal{A}}}$, and measures prediction error. Leave-one-benchmark-out validation holds out benchmark j and checks prediction accuracy.

H.1 Tests

Mardia [1970] proposed testing multivariate normality via the sample skewness and kurtosis. For M observations $\mathbf{x}_1, \dots, \mathbf{x}_M$ in \mathbb{R}^N with sample mean $\bar{\mathbf{x}}$ and covariance $\hat{\Sigma}$, define the squared Mahalanobis distance $d_{ij} = (\mathbf{x}_i - \bar{\mathbf{x}})^\top \hat{\Sigma}^{-1} (\mathbf{x}_j - \bar{\mathbf{x}})$. Mardia’s multivariate skewness and kurtosis are

$$\hat{\beta}_{1,N} = \frac{1}{M^2} \sum_{i,j=1}^M d_{ij}^3 \text{ and } \hat{\beta}_{2,N} = \frac{1}{M} \sum_{i=1}^M d_{ii}^2. \quad (21)$$

Under normality, $M\hat{\beta}_{1,N}/6 \xrightarrow{d} \chi_{N(N+1)(N+2)/6}^2$ and $\hat{\beta}_{2,N}$ is approximately normal with mean $N(N+2)$ and variance $8N(N+2)/M$. For univariate marginals, the Shapiro–Wilk test Shapiro and Wilk [1965] applied to each column of the residual matrix provides a per-benchmark normality check. Given the order statistics $x_{(1)} \leq \dots \leq x_{(M)}$ of a column, the test statistic is

$$W = \frac{(\sum_{i=1}^M a_i x_{(i)})^2}{\sum_{i=1}^M (x_i - \bar{x})^2}, \quad (22)$$

where the weights a_i are derived from the expected order statistics of a standard normal sample. Values of W close to 1 indicate normality; the null hypothesis is rejected for small W . Applying this test to each of the N residual columns (with a Bonferroni or Benjamini–Hochberg correction for multiple testing) flags individual benchmarks whose score distributions deviate from Gaussianity.

H.2 Results

We test normality using per-benchmark Shapiro–Wilk tests and Mardia’s multivariate skewness and kurtosis. Figure 12 summarises the results.

Univariate marginals. The Shapiro–Wilk test rejects normality for all 57 MMLU benchmarks and all 56 MTEB benchmarks (after Benjamini–Hochberg correction at $\alpha = 0.05$). Median W values are 0.84 (MMLU) and 0.89 (MTEB). The worst offenders on MMLU are multiple-choice subjects with highly discrete score distributions (marketing, $W = 0.66$; world_religions, $W = 0.70$), where accuracy values cluster at a few distinct levels. On MTEB, bimodal benchmarks like SprintDuplicateQuestions ($W = 0.46$) and STS17 ($W = 0.50$) are worst. For the MERGED matrix, 60 of 114 benchmarks reject and 54 pass; the smaller per-benchmark sample sizes (many columns have only 20–50 observed models) reduce the power of the test. The lowest W values are score benchmarks such as mmlu/world_religions ($W = 0.71$), mmlu/marketing ($W = 0.71$), and mmlu/logical_fallacies ($W = 0.74$).

Multivariate structure. Unsurprisingly, Mardia’s tests are equally negative. Details are omitted since the insights are redundant relative to the univariate marginals (for instance, $\hat{\beta}_{2,N} = 6,374$ versus the null expectation $N(N + 2) = 3,363$).

Implications. The formal rejection of Gaussianity is unsurprising: with $M = 5,452$ observations, even minor departures from normality are statistically detectable, and benchmark scores are bounded, discrete, and occasionally multimodal. The important question is whether these departures undermine the *practical* utility of the Gaussian imputation. The answer from the experiments is clearly no: the conditional mean $\hat{\mu}_{\bar{A}|A}$ is the best *linear* predictor of unobserved scores regardless of the true marginal distribution, and the R^2 values demonstrate that this linear predictor is highly effective. The Gaussian model should be understood as a convenient working approximation that provides both a principled selection criterion (via entropy or mutual information) and model-based uncertainty estimates, rather than a claim about the true data-generating process. Robustifying the imputation step, for instance via copula models or robust regression, is a natural direction for future work, but the present results suggest that the Gaussian framework already captures the dominant covariance structure that matters for benchmark selection.

I BenchPress

As an additional experiment, we apply our pipeline to the score matrix from the BenchPress project [BenchPress contributors, 2026], a recent effort to predict missing LLM benchmark scores via low-rank matrix completion. BenchPress assembles an 83×49 score matrix spanning 83 frontier models (from OpenAI, Anthropic, Google, Meta, DeepSeek, and others) across 49 benchmarks covering science, math, coding, reasoning, instruction following, and multimodal tasks. With only 33.8% of entries observed, this is the sparsest dataset in our study and presents a challenging test of covariance-based selection.

Greedy CV. Figure 13 shows the cross-validation results. At the 10% holdout (74 training models), greedy entropy selection achieves $R^2 \approx 0.21$ at $k = 5$ and $R^2 \approx 0.25$ at $k = 15$. Performance degrades sharply for larger holdout fractions: the 50% holdout yields negative R^2 at $k = 15$, and the 90% holdout (~ 8 training models for 49 benchmarks) is essentially uninformative. The random baseline (dashed lines) is competitive with greedy at all holdout levels, consistent with the heavily shrunk near-identity covariance. These results are comparable to the MERGED dataset, confirming that the sparse, rank-deficient regime ($M > N$ but 66% missing) limits the signal available for principled selection.

Entropy vs. MI. Figure 14 compares entropy, MI, and random selection at the 10% holdout. Entropy selection achieves the most stable R^2 (≈ 0.21 at $k = 5$), while MI selection is highly unstable, producing negative R^2 on several folds. This instability arises because the complement precision diagonal, which MI relies on via (9), is poorly estimated when the covariance is near-singular. Random selection ($R^2 \approx 0.24$ at $k = 5$) outperforms MI on average and is competitive with entropy. The residual variance and MI panels (center, right) show that entropy and MI do optimize their respective objectives, but this does not translate into better imputation in this data-poor regime.

Comparison with BenchPress methodology. The BenchPress project reports 7.25% median absolute percentage error using a blend of logit-space ridge regression and rank-2 SVD [BenchPress contributors, 2026]. Their approach differs from ours in two ways: (i) they operate in logit space, which handles the bounded nature of percentage scores, and (ii) they use all available entries for each prediction rather than selecting a fixed subset of benchmarks.

J Nonlinear Imputation via TabImpute

The Gaussian conditional mean used throughout this paper is the best *linear* predictor, but benchmark scores are bounded, discrete, and occasionally multimodal, suggesting that a nonlinear imputer might improve downstream R^2 . We use TABIMPUTE [Feitelberg et al., 2025], a pre-trained transformer for zero-shot tabular imputation, as an alternative imputation backend.

TABIMPUTE recasts imputation as in-context learning. Each cell (i, j) of the score matrix is featurized by concatenating its row, column, and position indices; observed cells serve as in-context training examples and missing cells as test queries. A 12-layer transformer with alternating between-feature and between-item attention processes these features and outputs a discretized probability distribution (5,000 bins) over each missing value. The model was pre-trained on approximately 25 million synthetic datasets generated from

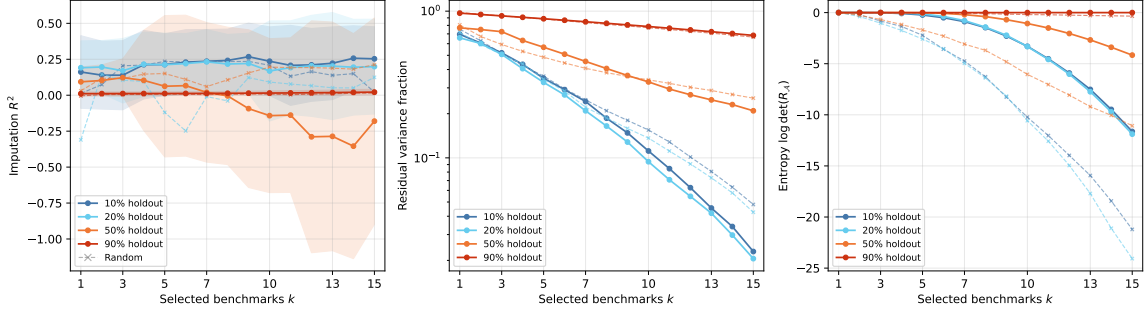


Figure 13: Cross-validation results for **BenchPress** (83×49 , 33.8% observed). Solid: greedy entropy; dashed: random baseline. Performance is comparable to the MERGED dataset, with $R^2 \approx 0.25$ at $k = 15$ under the 10% holdout.

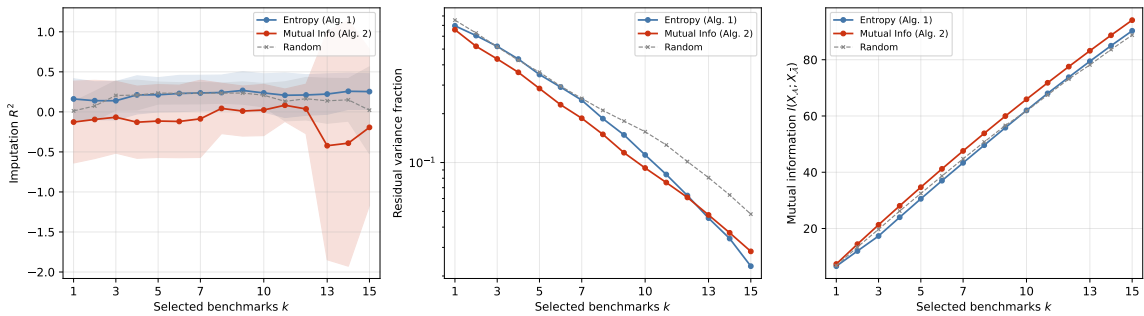


Figure 14: Entropy vs. MI vs. random selection on **BenchPress**. MI selection is unstable (negative R^2 on several folds) due to poorly estimated complement precision. Entropy and random selection achieve comparable $R^2 \approx 0.2$.

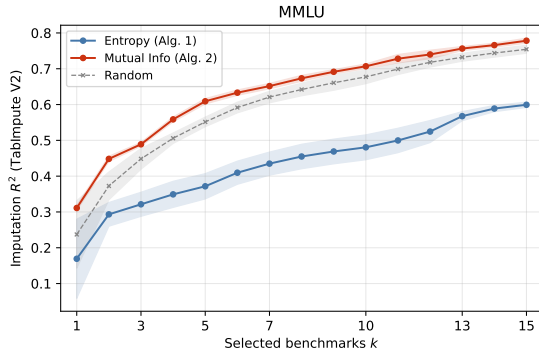
low-rank factor models $Y = UV^\top$ with diverse missingness patterns (MCAR, MAR, MNAR), requiring no fitting or hyperparameter tuning at inference time.

This architecture is well suited to our setting for two reasons. First, the low-rank factor model prior aligns with the empirical eigenspectrum of our score matrices (Section 5.2). Second, the zero-shot nature means we can swap the imputation step without modifying the upstream selection: after greedy or MI selection chooses a subset \mathcal{A} , we simply pass the partially observed row (selected benchmarks filled in, remainder NaN) to TABIMPUTE instead of computing the Gaussian conditional mean (6). We use the V2 architecture throughout, which removes the 50-column limit of the default model.

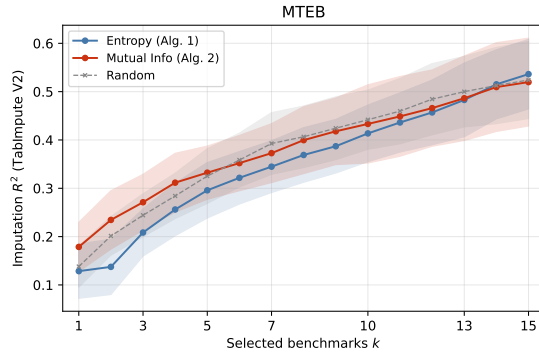
Experimental setup. We evaluate TABIMPUTE V2 as a drop-in replacement for Gaussian imputation under the same 10-fold CV protocol with 10% holdout used in Section 5.4. Benchmark selection (entropy, MI, random) is unchanged; only the imputation step differs. For each test model, a matrix is constructed with training rows (all observed entries retained as context) and the test row (only the k selected benchmarks revealed, remainder NaN). TABIMPUTE imputes the missing entries, and R^2 is computed in standardized space (per-benchmark z-score using training statistics) for comparability with the Gaussian results. For MMLU, where the training set exceeds 4,000 models, we subsample 3,800 training rows as context and process test models in batches of 200 to fit within GPU memory (12 GB). All other datasets fit without subsampling.

Results. Figures 15a–15d show the imputation R^2 for each selection method. Table 4 summarizes the results at $k = 5$ alongside the Gaussian baseline from Section 5.4.

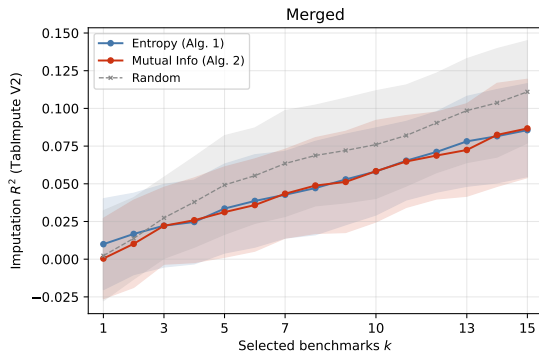
Gaussian imputation dominates TABIMPUTE on the main datasets, often by a factor of two or more. On MMLU, the Gaussian R^2 at $k = 5$ is 0.91 (MI selection) versus 0.61 for TABIMPUTE; on MTEB the gap is 0.76 versus 0.33. On the sparse MERGED dataset, TABIMPUTE is near zero while Gaussian imputation reaches $R^2 = 0.51$ with MI. BENCHPRESS remains difficult for both imputers; all $k = 5$ values are small, and the unstable MI-selected Gaussian baseline is negative.



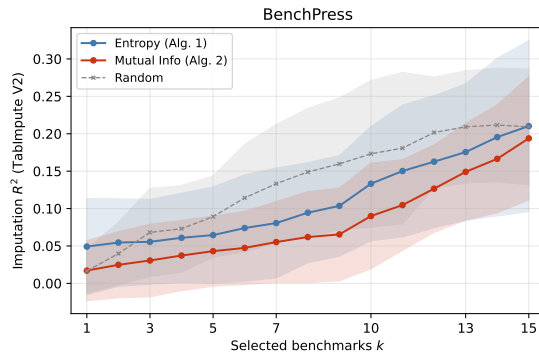
(a) MMLU. MI strongly dominates entropy and random, reaching $R^2 \approx 0.78$ at $k = 15$.



(b) MTEB. All three methods perform similarly, with MI slightly leading for small k .



(c) MERGED. Near-zero R^2 for all methods, reflecting the difficulty of zero-shot imputation on sparse data.



(d) BENCHPRESS. Entropy and random selection are comparable; MI remains unstable.

Figure 15: TABIMPUTE V2 imputation R^2 on all four datasets (10-fold CV, 10% holdout). Compare with Figures 5–7 (Gaussian imputation), where R^2 is substantially higher across the board.

Discussion. The Gaussian model’s advantage is not surprising: it estimates the covariance $\hat{\Sigma}$ from all training rows and exploits this structure directly in the conditional mean formula, which is the minimum-variance linear predictor. TABIMPUTE, by contrast, operates zero-shot: it was pre-trained on synthetic matrices with 10–50 rows and must infer the covariance structure from the in-context examples at inference time, without any dataset-specific parameter estimation. The comparison is therefore between an *adapted* linear model (Gaussian) and a *zero-shot* nonlinear model (TABIMPUTE).

Despite the lower overall R^2 , TABIMPUTE reveals an interesting pattern: MI selection outperforms entropy by a wide margin on MMLU (0.61 vs. 0.37), far more than under Gaussian imputation (0.91 vs. 0.89). This amplified gap occurs because entropy selects high-variance “outlier” benchmarks that are poorly connected to the majority, and TABIMPUTE’s nonlinear imputer cannot compensate for this lack of coupling as effectively as the Gaussian conditional mean (which explicitly uses the off-diagonal covariance entries). MI’s “hub” benchmarks provide TABIMPUTE with stronger in-context signal, partially closing the gap with the Gaussian baseline. These results suggest that the choice of selection objective matters more when the imputer is less powerful, reinforcing the practical importance of MI selection for budget-constrained evaluation.

K Logit-Space Score Transformation

Benchmark scores are often bounded (e.g., accuracy in $[0, 1]$), yet the Gaussian model assumes unbounded support. Inspired by the logit-space transformation used in the BenchPress project [BenchPress contributors, 2026], we investigate whether working in logit space improves imputation quality.

Transformation. For each benchmark j , let $s_{\max,j}$ be the maximum observed score in the training set. We normalize scores to $[0, 1]$ via $\tilde{s}_{ij} = s_{ij}/s_{\max,j}$, clip to $[\varepsilon, 1 - \varepsilon]$ with $\varepsilon = 10^{-3}$, and apply the logit transform

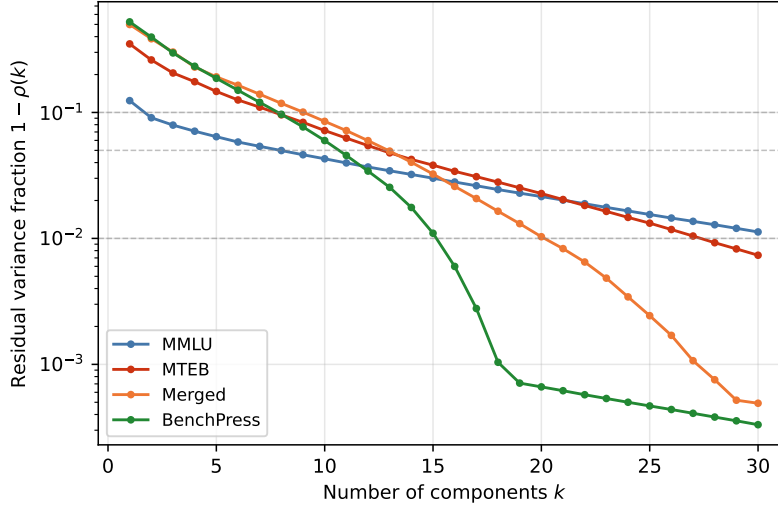


Figure 16: Residual variance of the logit-transformed correlation matrix. Compare with Figure 1 (raw scores). Logit space is slightly less compressible.

$f_{ij} = \log(\tilde{s}_{ij}/(1 - \tilde{s}_{ij}))$. All downstream steps, covariance estimation, benchmark selection, and Gaussian conditional imputation, operate on f_{ij} . Predictions are inverted via $\hat{s}_{ij} = \sigma(\hat{f}_{ij}) \cdot s_{\max,j}$, and R^2 is computed in raw-score space (standardized using training statistics) for direct comparability with the results in Section 5. This inverse map caps predictions at the training-set maximum, which can hurt extrapolation to stronger validation models.

Eigenspectrum. Figure 16 shows the residual variance of the logit-transformed correlation matrices. The spectra are similar to the raw-score versions (Figure 1): MMLU reaches 90% explained variance at $k = 2$ (unchanged), while MTEB requires $k = 8$ (vs. 6 in raw space) and MERGED requires $k = 10$ (vs. 8). The logit transform slightly increases the effective dimensionality, likely because it stretches the tails of the score distribution.

Imputation results. Table 5 compares MI-selected imputation R^2 at $k = 5$ between raw-score and logit-space pipelines. On MMLU, the two are nearly identical (0.91). On all other datasets, the logit transform *reduces* R^2 : from 0.76 to 0.72 on MTEB, from 0.51 to 0.39 on MERGED, and from -0.11 to -0.22 on BENCHPRESS.

Discussion. The logit transform does not improve imputation on any dataset. Several factors explain this. First, the Gaussian conditional mean is the best linear predictor regardless of the marginal distribution, so the Gaussianity argument for logit is weaker than it appears. Second, the 0-max normalization assumes comparable non-negative score scales, while the heterogeneous MERGED matrix still combines accuracies, win rates, judge scores, and benchmark-specific ratings. Third, the logit transform compresses mid-range scores and stretches extremes, while the inverse map caps predictions at s_{\max} ; together these effects can amplify noise near the boundaries and penalize validation models that exceed the training maximum. These findings are consistent with the observation that the raw Gaussian framework is already a strong working approximation for the dominant linear structure of benchmark score matrices.

Figures 17 and 18 show the full CV curves and entropy-vs-MI comparisons in logit space.

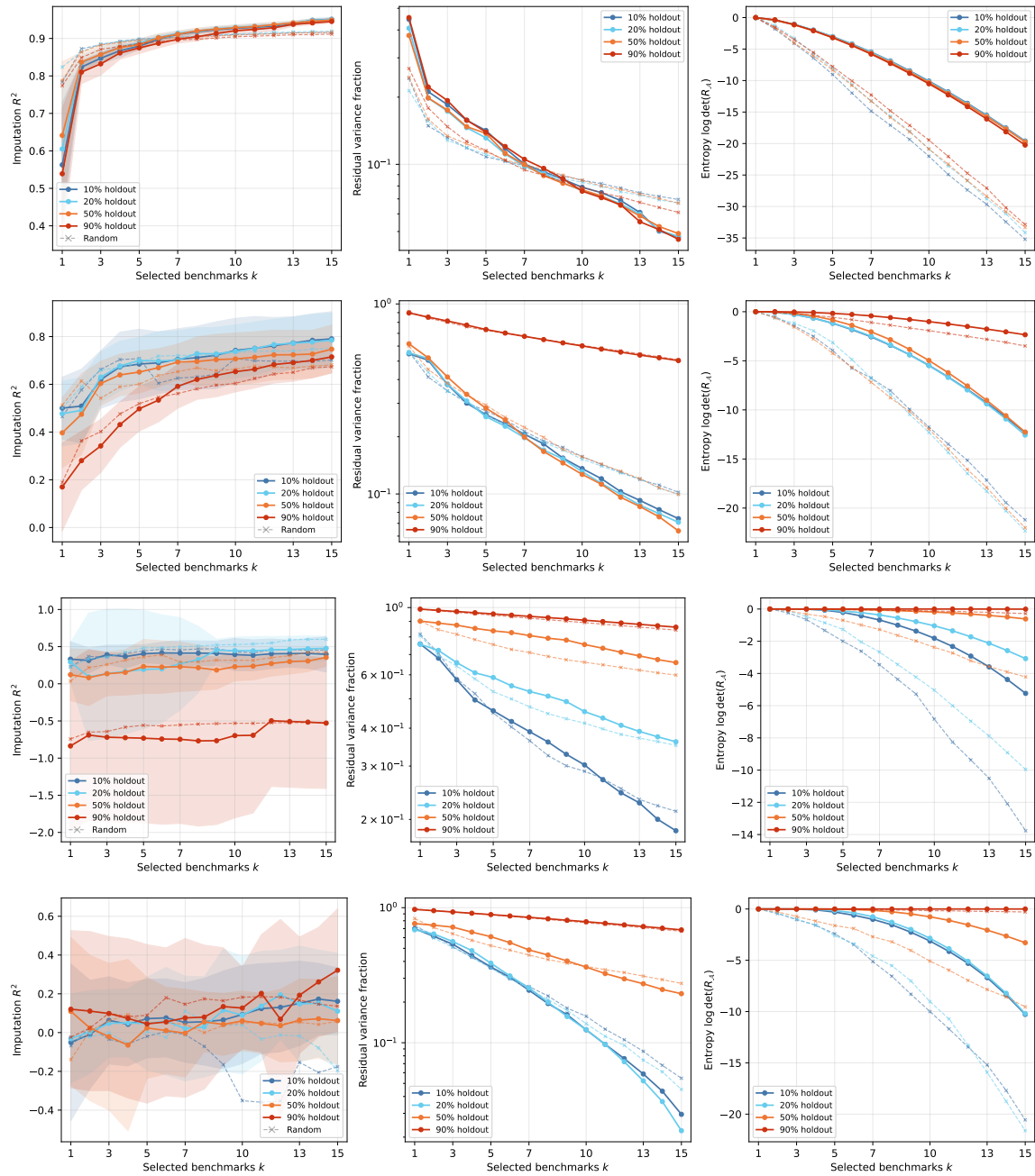


Figure 17: Greedy entropy CV in logit space (solid: greedy, dashed: random) for MMLU, MTEB, MERGED, and BENCHPRESS (top to bottom). Compare with Figures 2–4 (raw scores).

Table 3: Number of models per collection that could not be matched to any other collection. Full lists are provided below.

| Collection | Total | Unmatched |
|--------------|-------|-----------|
| MMLU | 5454 | 5424 |
| Open LLM v2 | 4507 | 4450 |
| HELM Lite | 30 | 13 |
| AlpacaEval 2 | 223 | 166 |
| Arena-Hard | 60 | 10 |
| LiveBench | 195 | 121 |
| WildBench | 63 | 15 |
| MT-Bench | 5 | 2 |
| BigCodeBench | 155 | 94 |
| MTEB | 268 | 268 |

Table 4: Imputation R^2 at $k = 5$ for Gaussian conditional mean vs. TABIMPUTE V2, under entropy, MI, and random selection (10-fold CV, 10% holdout). The better imputer for each dataset/objective pair is bolded.

| Dataset | Entropy | | MI | | Random | |
|------------|-------------|--------|-------------|-------------|-------------|--------|
| | Gauss | TabImp | Gauss | TabImp | Gauss | TabImp |
| MMLU | 0.89 | 0.37 | 0.91 | 0.61 | 0.89 | 0.55 |
| MTEB | 0.72 | 0.30 | 0.76 | 0.33 | 0.76 | 0.33 |
| MERGED | 0.35 | 0.03 | 0.51 | 0.03 | 0.53 | 0.05 |
| BENCHPRESS | 0.21 | 0.06 | -0.11 | 0.04 | 0.24 | 0.09 |

Table 5: Imputation R^2 at $k = 5$ (10-fold CV, 10% holdout): raw-score vs. logit-space Gaussian imputation. All values use MI selection.

| Dataset | Raw | Logit |
|------------|--------------|-------|
| MMLU | 0.91 | 0.91 |
| MTEB | 0.76 | 0.72 |
| MERGED | 0.51 | 0.39 |
| BENCHPRESS | -0.11 | -0.22 |

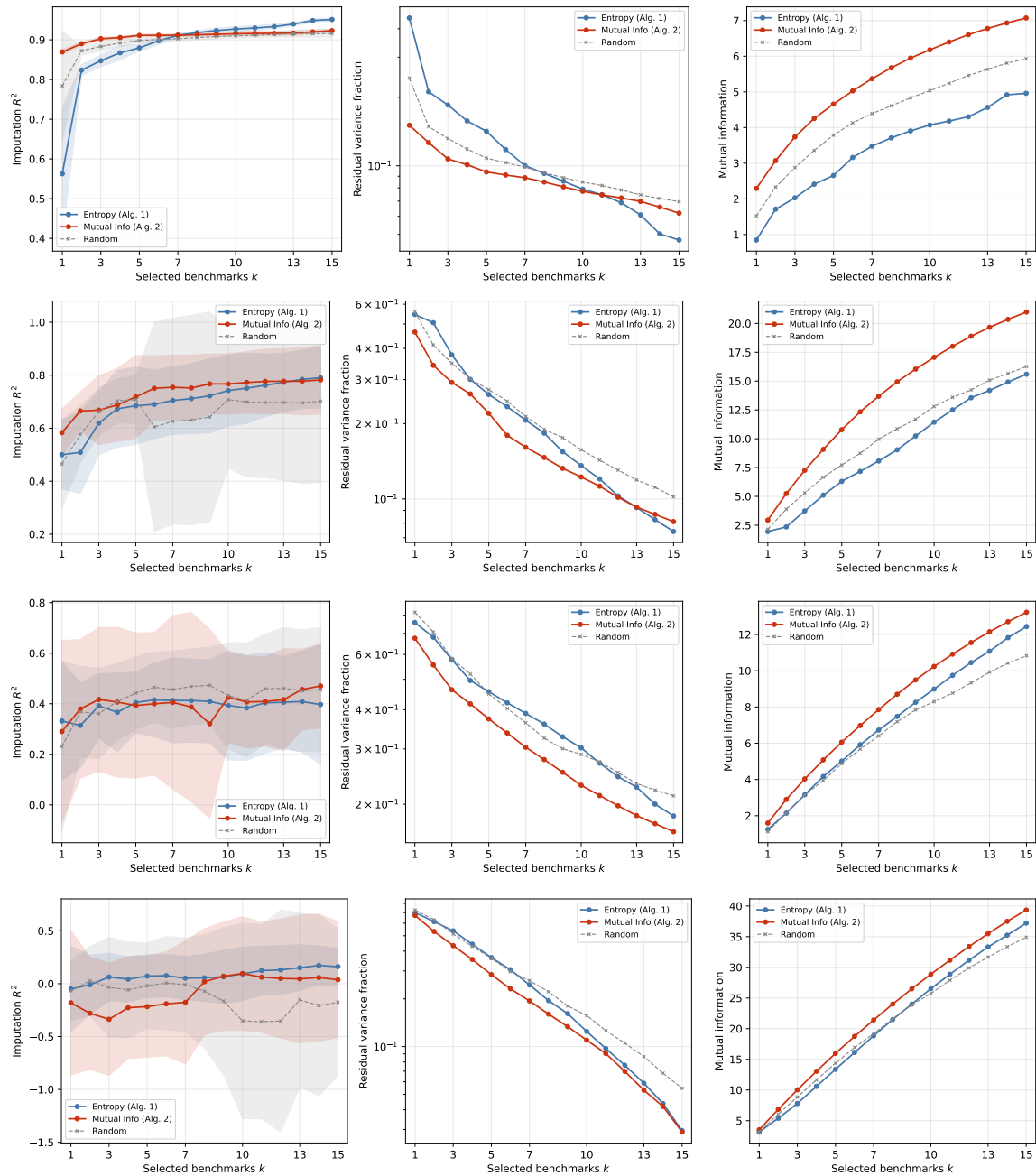


Figure 18: Entropy vs. MI vs. random selection in logit space (10-fold CV, 10% holdout) for MMLU, MTEB, MERGED, and BENCHPRESS (top to bottom). Compare with Figures 5–7 (raw scores).